National Institute of Allergy and Infectious Diseases

Malcolm A. Martin, M.D.

Chief, Laboratory of Molecular Microbiology
Chief, Viral Pathogenesis and Vaccine Section
Contact Information
Malcolm A. Martin, M.D. (https://ned.nih.gov/search/ViewDetails.aspx?NIHID=0010191068)

Malcolm A. Martin, M.D.

Credit: NIAID

Major Areas of Research

- Studies of primate and murine retroviral biology and genetics in cell culture systems and animal models
- Assessment of the SIV and SIV/HIV chimeric virus (SHIV) acute infections in macaque monkeys
- Development of R5-tropic SHIVs as challenge viruses in vaccine experiments
- Use of R5-tropic SHIVs to investigate the development of cross-reacting anti-HIV-1 neutralizing antibodies in virus-infected and vaccinated nonhuman primate models of HIV/AIDS

Program Description

The Viral Pathogenesis and Vaccine Section (VPVS) develops and uses SIV and SIV/HIV chimeric viruses (SHIVs) as surrogates of HIV-1 to investigate virus-induced immunopathogenesis and to develop effective prophylactic vaccines in nonhuman primate models. Toward this end, we have constructed X4- and R5-tropic SHIVs that durably infect macaques and cause systemic depletion of CD4+ T cells in rhesus monkeys, resulting in clinical disease. Recent work has focused on 1) recombination-mediated changes in co-receptor utilization that confer an augmented pathogenic phenotype and 2) the development of cross-reacting neutralizing antibodies directed against the HIV-1 envelope glycoproteins in animals inoculated with the R5-tropic SHIVAD8.

Recent Results

Intermolecular recombination between HIV-1 strains circulating in an infected individual is now recognized to be a major mechanism involved in the emergence of drug-resistant and immunological escape variants. HIV-1 recombination has been studied *in vivo* by inoculating individual rhesus macaques with X4- and R5-tropic SHIVs. In one of the infected monkeys, both SHIVs were potently suppressed by week 12 post-inoculation, but a burst of viremia at week 51 was accompanied by an unrelenting loss of total CD4+ T cells and the development of clinical disease (Fig. 1A). PCR analyses of plasma viral RNA indicated an *env* gene segment, containing the V3 region from the inoculated X4 SHIV, had been transferred into the genetic background of the input R5 SHIV by intergenomic recombination, creating an X4 virus with novel replicative, serological, and pathogenic properties (Fig. 1B). These results indicate that the effects of retrovirus recombination *in vivo* can be functionally profound and may even occur when one of the recombination participants is undetectable in the circulation as cell-free virus.

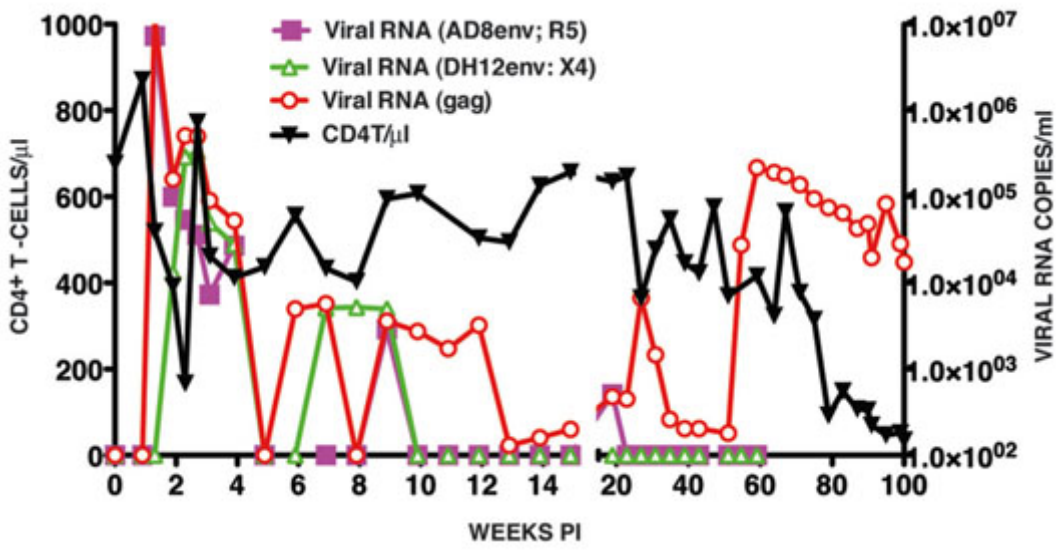

Figure 1: Timeline of recombination events occurring in a rhesus monkey following the inoculation of X4 and R5 SHIVs.
A. Levels of plasma viral RNA and CD4+ T cells in the dually infected animal.

Credit: NIAID

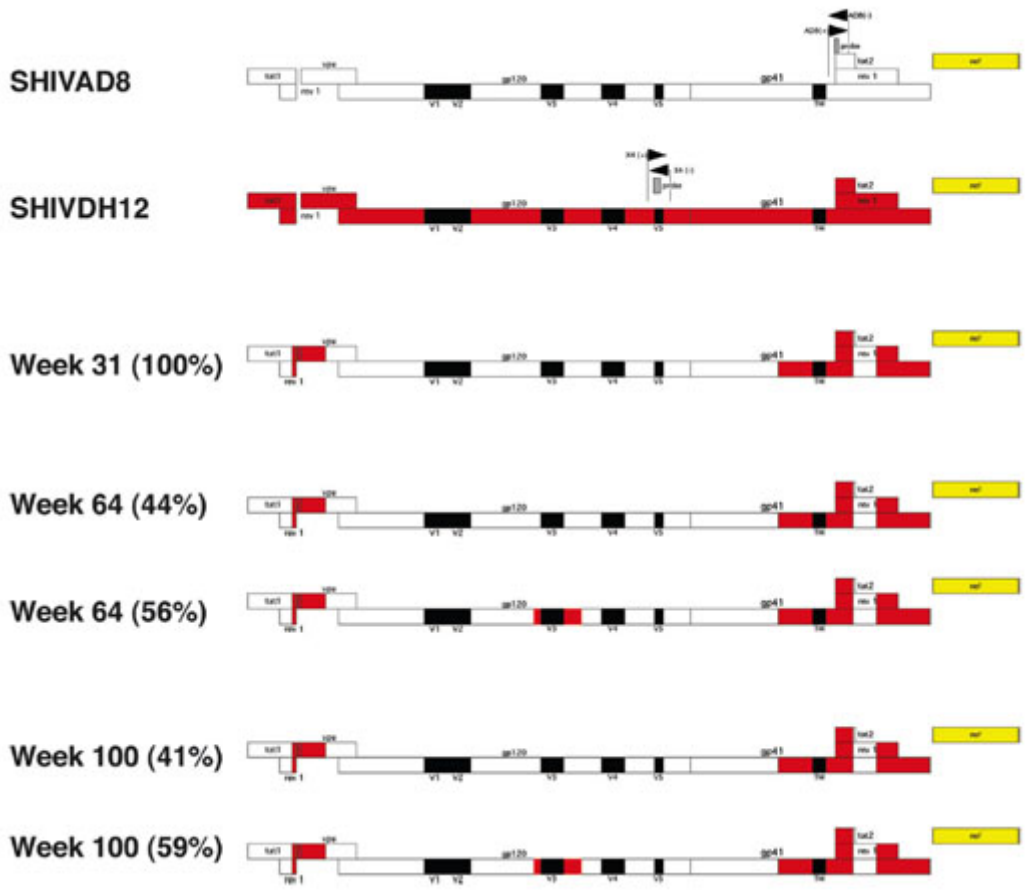

Figure 1: Timeline of recombination events occurring in a rhesus monkey following the inoculation of X4 and R5 SHIVs.
B. Composition of envelope genes in the plasma virus(es) present following infection.

Credit: NIAID

An R5-tropic SHIV that causes gradual losses of both memory and naïve CD4+ T lymphocytes, generates anti-viral CD4+ and CD8+ T-cell responses, and generates sustained chronic immune activation while maintaining variable levels of plasma viremia (102 to 105 RNA copies/ml for up to three years post-innoculation) and death from immunodeficiency has been generated (Fig 2).

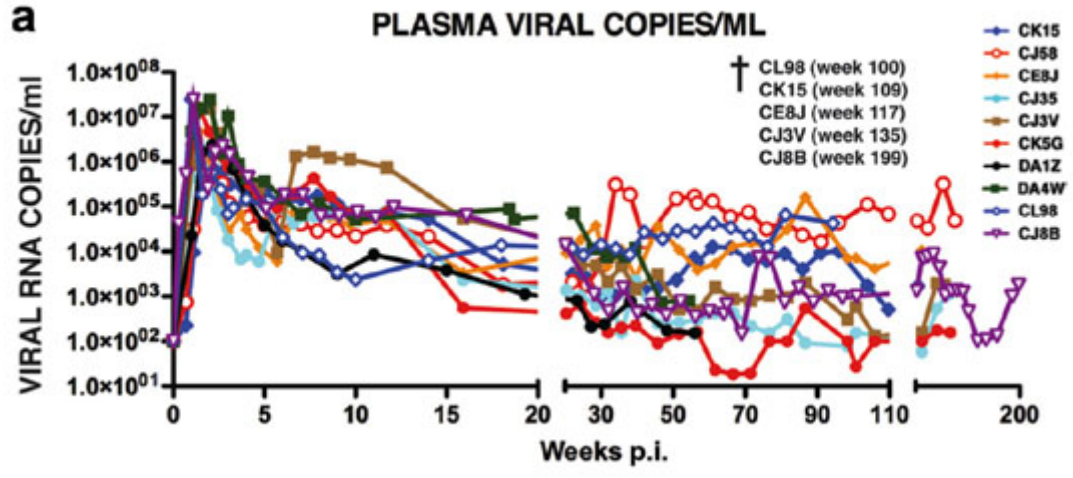

Figure 2A. Plasma Viral Copies / ML

Credit: NIAID

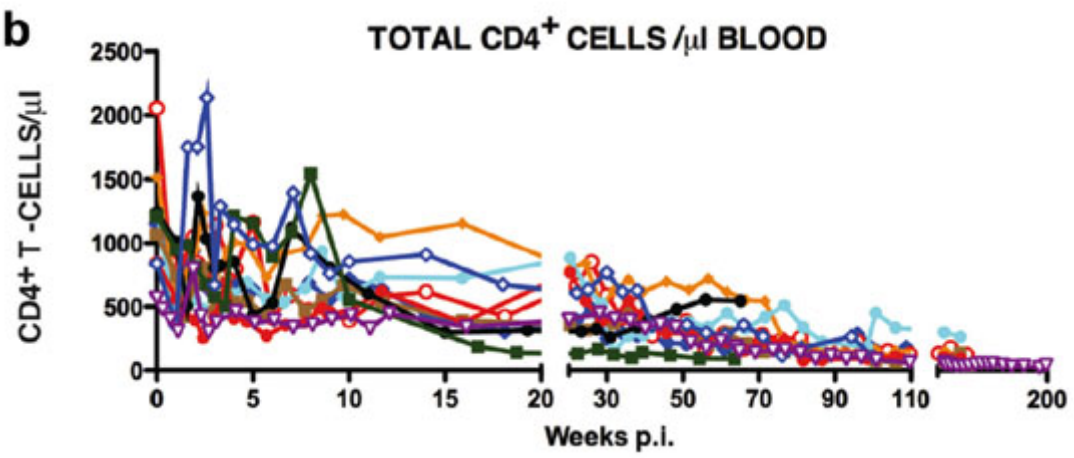

Figure 2: The levels of plasma viremia (a) and absolute numbers of peripheral CD4+ T lymphocytes (b) in rhesus macaques inoculated intravenously with the R5-tropic $SHIV_{AD8}$.

SHIVs express the HIV envelope glycoprotein and can therefore be used to evaluate HIV-1 Env specific neutralizing antibody (NAb) responses. Developing an SHIV that is capable of eliciting broad and potent NAb responses and tracking the evolution of this immune response might provide unprecedented insight into the factors associated with the development of bNAbs.

Plasma from 14 R5-tropic SHIV-infected macaques was therefore screened for the presence of high-titered broadly reacting neutralizing activity, and a single macaque (Rh CE8J) with potent cross-clade plasma NAb response was identified (Fig. 3). Neutralization assays were carried out using samples taken at serial time points and indicated that the development of broad plasma neutralization was unusually rapid and coincided with the development of autologous NAbs. Furthermore, serum mapping studies suggested that the bNAbs interact with carbohydrates and are critically dependent on the N332 glycan (Fig. 4).

weeks post infection	score	JR-CSF	MGRM-C26	92RW020	YU2	92BR020	JR-FL	94UG103	92TH021	$SHIV_{AD8}$	SIVmac239 (neg. control)
20	0.37	<100	<100	<100	<100	<100	<100	<100	<100	<100	<100
24	0.37	<100	<100	<100	<100	<100	<100	<100	<100	<100	<100
29	0.37	<100	<100	<100	100	<100	<100	<100	<100	<100	<100
32	0.91	100	<100	<100	350	400	<100	<100	<100	450	<100
36	1.76	<100	805	250	1684	1880	100	<100	<100	811	<100
40	2.28	<100	1600	1337	1014	>2700	1066	<100	<100	3282	<100
46	2.70	250	>2700	>2700	1500	>2700	1657	<100	<100	2873	<100
52	2.75	735	>2700	>2700	1261	>2700	1063	<100	<100	1899	<100
57	2.60	400	>2700	>2700	900	>2700	735	<100	<100	1709	<100
60	2.57	300	>2700	2134	1300	>2700	640	<100	<100	1324	<100
67	2.69	960	>2700	>2700	800	>2700	760	<100	<100	1181	<100
72	2.75	1456	>2700	>2700	870	>2700	740	<100	<100	1907	<100
77	3.28	>2700	>2700	>2700	1800	>2700	>2700	400	<100	5193	<100
80	2.54	1336	1586	>2700	400	1901	720	<100	<100	1181	<100
86	2.31	1002	735	2495	200	2007	550	<100	<100	510	<100
101	2.22	1173	640	2343	250	>2700	450	<100	<100	397	<100
115	2.57	1095	1050	>2700	350	>2700	1295	<100	<100	1106	<100

Figure 3: Development of potent broadly cross-clade neutralizing antibodies directed against heterologous HIV-1 strains by a macaque (Rh CE8J) inoculated with the R5-tropic SHIVAD8. Titers in each cell are color coded as follows: gray, IC50 <1:100; green, 1:100< IC50 <1:300; yellow, 1:300< IC50 <1:500; orange, 1:500< IC50 <1:1000; red, IC50 >1:1000.

Credit: NIAID

weeks post infection	JR-FL	JR-FL N332A	MGRM-C26	MGRM-C26 N332A
20	<100	<100	<100	<100
24	<100	<100	<100	<100
29	<100	<100	<100	<100
32	<100	<100	<100	<100
36	100	<100	805	<100
40	1066	<100	1600	<100
46	1657	<100	>2700	<100
52	1063	<100	>2700	<100
57	735	<100	>2700	<100
60	640	<100	>2700	<100
67	760	<100	>2700	<100
72	740	<100	>2700	<100
77	>2700	<100	>2700	<100
80	720	<100	1586	<100
86	550	<100	735	<100
101	450	<100	640	<100
115	1295	<100	1050	<100

weeks post infection	$SHIV_{AD8}$	$SHIV_{AD8}$ N332A
20	<100	<100
24	<100	<100
29	<100	<100
32	450	<100
36	811	<100
40	3282	300
46	2873	100
52	1899	300
57	1709	100
60	1324	200
67	1181	<100
72	1907	<100
77	5193	<100
80	1181	<100
86	510	<100
101	397	100
115	1106	<100

Figure 4: The cross-reacting anti-HIV-1 neutralizing activity generated in macaque CE8J is directed against the gp120 N332 glycan epitope. Plasma samples collected at serial time points were tested for neutralizing activity against JR-CSF, MGRM-C26, and SHIVAD8 pseudovirus variants containing an N332A mutation. Cells are color coded as follows: gray, IC50 <1:100; green, 1:100< IC50 <1:300; yellow, 1:300< IC50 <1:600; orange, 1:600< IC50 <1:1000; red, IC50 >1:1000.

Credit: NIAID

Biography

Dr. Martin received an M.D. from Yale University School of Medicine in 1962 and, following two years of clinical training in internal medicine at the University of Rochester, joined NIH as a research associate. He initially investigated the replication and gene regulation of SV40 and polyomaviruses and subsequently studied endogenous murine and human retroviral sequences. Since 1984, his research program has focused on HIV. Dr. Martin was appointed chief of the Laboratory of Molecular Microbiology when it was established in 1981. He is a member of the National Academy of Sciences and the recipient of numerous scientific awards.

Memberships

- Elected to The National Academy of Sciences, 1998
- Elected to The American Academy of Microbiology, 1998
- ISI Highly Cited Researcher

Editorial Boards

- *Journal of Virology*

- Associate Editor, *Fields Virology*, Fourth, Fifth and Sixth Editions, 2001-2012
- Scientific Advisory Committee, New England Regional Primate Center

Research Group

Yoshiaki Nishimura, Ph.D., Staff Scientist
Bernard Lafont, Ph.D., Staff Scientist
Rajeev Gautam, Ph.D., Staff Scientist
Masashi Shingai, Ph.D., Research Fellow
Wendy Lee, B.S., Biologist
Olivia Donau, B.A., Biologist
Reza Sadjadpour, M.S., Biologist

Selected Publications

Gautam R, Nishimura Y, Lee WR, Donau O, Buckler-White A, Shingai M, Sadjadpour R, Schmidt SD, LaBranche CC, Keele BF, Montefiori D, Mascola JR, Martin MA. Pathogenicity and mucosal transmissibility of the R5-tropic simian/human immunodeficiency virus SHIV(AD8) in rhesus macaques: implications for use in vaccine studies. (http://www.ncbi.nlm.nih.gov/pubmed/22647691) *J Virol*. 2012 Aug;86(16):8516-26.

Walker LM, Sok D, Nishimura Y, Donau O, Sadjadpour R, Gautam R, Shingai M, Pejchal R, Ramos A, Simek MD, Geng Y, Wilson IA, Poignard P, Martin MA, Burton DR. Rapid development of glycan-specific, broad, and potent anti-HIV-1 gp120 neutralizing antibodies in an R5 SIV/HIV chimeric virus infected macaque. (http://www.ncbi.nlm.nih.gov/pubmed/22123961) *Proc Natl Acad Sci U S A*. 2011 Dec 13;108(50):20125-9.

Shingai M, Yoshida T, Martin MA, Strebel K. Some human immunodeficiency virus type 1 Vpu proteins are able to antagonize macaque BST-2 *in vitro* and *in vivo*: Vpu-negative simian-human immunodeficiency viruses are attenuated *in vivo*. (http://www.ncbi.nlm.nih.gov/pubmed/21775449) *J Virol*. 2011 Oct;85(19):9708-15.

Nishimura Y, Martin MA. The acute HIV infection: implications for intervention, prevention and development of an effective AIDS vaccine. (http://www.ncbi.nlm.nih.gov/pubmed/21909345) *Curr Opin Virol*. 2011 Sep;1(3):204-10.

Nishimura Y, Shingai M, Lee WR, Sadjadpour R, Donau OK, Willey R, Brenchley JM, Iyengar R, Buckler-White A, Igarashi T, Martin MA. Recombination-mediated changes in coreceptor usage confer an augmented pathogenic phenotype in a nonhuman primate model of HIV-1-induced AIDS. (http://www.ncbi.nlm.nih.gov/pubmed/21813599) *J Virol*. 2011 Oct;85(20):10617-26.

Nishimura Y, Shingai M, Willey R, Sadjadpour R, Lee WR, Brown CR, Brenchley JM, Buckler-White A, Petros R, Eckhaus M, Hoffman V, Igarashi T, Martin MA. Generation of the pathogenic R5-tropic simian/human immunodeficiency virus SHIVAD8 by serial passaging in rhesus macaques. (http://www.ncbi.nlm.nih.gov/pubmed/20147396) *J Virol*. 2010 May;84(9):4769-81.

Visit PubMed for a complete publication listing. (http://www.ncbi.nlm.nih.gov/sites/entrez?cmd=search&db=pubmed&term=%28martin%20ma%5bauth%5d%20%29%20and%20%28hiv%5btitle/abstract%5d%20or%20shiv%5btitle/

Patents

Martin MA, Willey R, inventors; The United States of America as represented by the Department of Health, assignee. Non-infectious mutant clone of HIV. (http://patft.uspto.gov/netacgi/nph-Parser?Sect1=PTO1&Sect2=HITOFF&d=PALL&p=1&u=/netahtml/PTO/srchnum.htm&r=1&f=G&l=50&s1=4%2c931%2c393.PN.&OS=PN/4%2c931 States patent US 4,931,393. 5 Jun 1990.

Folks TM, Powell D, Malcolm MA, inventors; The United States of America as represented by the Department of Health, assignee.Cell line producing AIDS viral antigens without producing infectious virus particles. (http://patft.uspto.gov/netacgi/nph-Parser?Sect1=PTO1&Sect2=HITOFF&d=PALL&p=1&u=/netahtml/PTO/srchnum.htm&r=1&f=G&l=50&s1=4%2c752%2c565.PN.&OS=PN/4%2c752 States patents US 4,752,565. 21 Jun 1988.

Content last reviewed on March 14, 2014

Federal Employee Profile — Malcolm A. Martin

Malcolm A. Martin

Title: Medical Officer (Job titles are sourced from the OPM. Keep in mind that the OPM has a limited set of job classifications with which to describe a wide variety of employees, so in some cases a generic job classification will be used if a more specific one is not available.)

Agency: National Institutes of Health

In 2018, Malcolm A. Martin was a Medical Officer at the National Institutes of Health in Bethesda, Maryland. As our dataset only goes as far back as 2004, it is likely that has worked in the federal government prior to 2004.

Malcolm A. Martin is a RF-00 under the code is for use by hhs only. payscale and is among the **highest-paid ten percent of employees** in the National Institutes of Health.

Year	Occupation	Paygrade	Base Salary	Bonus	Location
2018	Medical Officer	RF-00	$262,650	$0	Bethesda, Maryland
2017	Medical Officer	RF-00	$262,650	$0	Bethesda, Maryland
2016	Medical Officer	RF-00	$257,500	$0	Bethesda, Maryland
2015	Medical Officer	AD-00	$248,865	$0	Bethesda, Maryland
2014	Medical Officer	AD-00	$239,293	$0	Bethesda, Maryland
2013	Medical Officer	AD-00	$239,293	$0	Bethesda, Maryland
2012	Medical Officer	AD-00	$239,293	$0	Bethesda, Maryland
2011	Medical Officer	AD-00	$239,293	$0	Bethesda, Maryland
2010	Medical Officer	AD-00	$239,293	$0	Bethesda, Maryland
2009	Medical Officer	AD-00	$234,601	$0	Bethesda, Maryland
2008	Medical Officer	AD-00	$230,001	$0	Bethesda, Maryland
2007	Medical Officer	AD-00	$211,926	$1,500	Bethesda, Maryland
2006	Medical Officer	AD-00	$209,000	$0	Bethesda, Maryland
2005	Medical Officer	AD-00	$201,778	$0	Bethesda, Maryland
2004	Medical Officer	AD-00	$194,017	$0	Bethesda, Maryland

FederalPay's Employee Information Policy

Federal employees' salaries are considered public information under 5 U.S.C. § 552, and in the interest of government transparency FederalPay publishes the salary information of all federal employees who earn more than $100,000 per year, or who are in the highest paid 10% of their agency. This data is published unmodified, as provided by the OPM.

Run a people search on Malcolm A. Martin

Search National Institutes of Health Employees

Employee Statistics

Malcolm A. Martin's 2018 pay is

↑ 108%

higher than the average Medical Officer across all agencies.

Malcolm A. Martin's 2018 pay is

↑ 29%

higher than the average pay of a RF employee at the National Institutes of Health.

Malcolm A. Martin's pay trend during his or her government career in the National Institutes of Health:

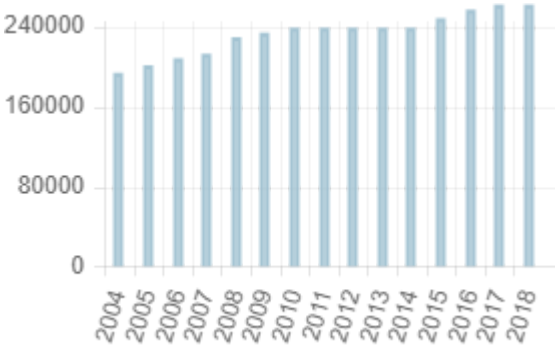

Data Sources

The information provided on these pages is sourced from the Office of Personnel Management (OPM) Enterprise Human Resources Integration (EHRI) dataset. Postal Service data is managed exclusively by the USPS. All information is displayed unmodified and as provided by the source agency.

Federal employee salaries are public information under open government laws (5 U.S.C. § 552). FederalPay provides this data in the interest of government transparency — employee data may not be used for commercial soliciting or vending of any kind. Learn more about the FederalPay Employees Dataset here.

NIH Intramural Research Program
Our Research Changes Lives

Malcolm A. Martin, M.D.

NIH Distinguished Investigator

Viral Pathogenesis and Vaccine Section

NIAID/DIR

VIEW SITE (https://www.niaid.nih.gov/node/3146)

Building 4, Room 315
4 Memorial Drive
Bethesda, MD 20892

301-496-4012

mmartin@niaid.nih.gov

Research Topics

The Viral Pathogenesis and Vaccine Section (VPVS) develops and uses SIV and SIV/HIV chimeric viruses (SHIVs) as surrogates of HIV-1 to investigate virus-induced immunopathogenesis and to develop effective prophylactic vaccines in nonhuman primate models. Toward this end, we have constructed X4- and R5-tropic SHIVs that durably infect macaques and cause systemic depletion of CD4+ T cells in rhesus monkeys, resulting in clinical disease. Recent work has focused on 1) recombination-mediated changes in co-receptor utilization that confer an augmented pathogenic phenotype and 2) the development of cross-reacting neutralizing antibodies directed against the HIV-1 envelope glycoproteins in animals inoculated with the R5-tropic SHIVAD8.

Recent Results

Intermolecular recombination between HIV-1 strains circulating in an infected individual is now recognized to be a major mechanism involved in the emergence of drug-resistant and immunological escape variants. HIV-1 recombination has been studied *in vivo* by inoculating individual rhesus macaques with X4- and R5-tropic SHIVs. In one of the infected monkeys, both SHIVs were potently suppressed by week 12 post-inoculation, but a burst of viremia at week 51 was accompanied by an unrelenting loss of total CD4+ T cells and the development of clinical disease (Fig. 1A). PCR analyses of plasma viral RNA indicated an *env* gene segment, containing the V3 region from the inoculated X4 SHIV, had been transferred into the genetic background of the input R5 SHIV by intergenomic recombination, creating an X4 virus with novel replicative, serological, and pathogenic properties (Fig. 1B). These results indicate that the effects of retrovirus recombination *in vivo* can be functionally profound and may even occur when one of the recombination participants is undetectable in the circulation as cell-free virus.

Timeline of recombination events occurring in a rhesus monkey following the inoculation of X4 and R5 SHIVs.

Figure 1A

Composition of envelope genes in the plasma virus(es) present following infection.

Figure 1B
Figure 1: Timeline of recombination events occurring in a rhesus monkey following the inoculation of X4 and R5 SHIVs. A. Levels of plasma viral RNA and CD4+ T cells in the dually infected animal. B. Composition of envelope genes in the plasma virus(es) present following infection.

An R5-tropic SHIV that causes gradual losses of both memory and naïve CD4+ T lymphocytes, generates anti-viral CD4+ and CD8+ T-cell responses, and generates sustained chronic immune activation while maintaining variable levels of plasma viremia (102 to 105 RNA copies/ml for up to three years post-innoculation) and death from immunodeficiency has been generated (Fig 2).

Plasma Viral Copies / ML Total CD4+ Cells/jul Blood

Figure 2: The levels of plasma viremia (a) and absolute numbers of peripheral CD4+ T lymphocytes (b) in rhesus macaques inoculated intravenously with the R5-tropic SHIVAD8.

SHIVs express the HIV envelope glycoprotein and can therefore be used to evaluate HIV-1 Env specific neutralizing antibody (NAb) responses. Developing an SHIV that is capable of eliciting broad and potent NAb responses and tracking the evolution of this immune response might provide unprecedented insight into the factors associated with the development of bNAbs. Plasma from 14 R5-tropic SHIV-infected macaques was therefore screened for the presence of high-titered broadly reacting neutralizing activity, and a single macaque (Rh CE8J) with potent cross-clade plasma NAb response was identified (Fig. 3). Neutralization assays were carried out using samples taken at serial time points and indicated that the development of broad plasma neutralization was unusually rapid and coincided with the development of autologous NAbs. Furthermore, serum mapping studies suggested that the bNAbs interact with carbohydrates and are critically dependent on the N332 glycan (Fig. 4).

Development of potent broadly cross-clade neutralizing antibodies directed against heterologous HIV-1 strains by a macaque (Rh CE8J) inoculated with the R5-tropic SHIVAD8.

Figure 3: Development of potent broadly cross-clade neutralizing antibodies directed against heterologous HIV-1 strains by a macaque (Rh CE8J) inoculated with the R5-tropic SHIVAD8. Titers in each cell are color coded as follows: gray, IC50 <1:100; green, 1:100< IC50 <1:300; yellow, 1:300< IC50 <1:500; orange, 1:500< IC50 <1:1000; red, IC50 >1:1000.

The cross-reacting anti-HIV-1 neutralizing activity generated in macaque CE8J is directed against the gp120 N332 glycan epitope.

Figure 4: The cross-reacting anti-HIV-1 neutralizing activity generated in macaque CE8J is directed against the gp120 N332 glycan epitope. Plasma samples collected at serial time points were tested for neutralizing activity against JR-CSF, MGRM-C26, and SHIVAD8 pseudovirus variants containing an N332A mutation. Cells are color

coded as follows: gray, IC50 <1:100; green, 1:100< IC50 <1:300; yellow, 1:300< IC50 <1:600; orange, 1:600< IC50 <1:1000; red, IC50 >1:1000.

Biography

Dr. Martin received an M.D. from Yale University School of Medicine in 1962 and, following two years of clinical training in internal medicine at the University of Rochester, joined NIH as a research associate. He initially investigated the replication and gene regulation of SV40 and polyomaviruses and subsequently studied endogenous murine and human retroviral sequences. Since 1984, his research program has focused on HIV. Dr. Martin was appointed chief of the Laboratory of Molecular Microbiology when it was established in 1981. He is a member of the National Academy of Sciences and the recipient of numerous scientific awards.

Memberships

- Elected to The National Academy of Sciences, 1998
- Elected to The American Academy of Microbiology, 1998
- ISI Highly Cited Researcher

Editorial Boards

- *Journal of Virology*
- Associate Editor, *Fields Virology*, Fourth, Fifth and Sixth Editions, 2001-2012
- Scientific Advisory Committee, New England Regional Primate Center

Selected Publications

1. Shingai M, Nishimura Y, Klein F, Mouquet H, Donau OK, Plishka R, Buckler-White A, Seaman M, Piatak M Jr, Lifson JD, Dimitrov DS, Nussenzweig MC, Martin MA. Antibody-mediated immunotherapy of macaques chronically infected with SHIV suppresses viraemia. (https://www.ncbi.nlm.nih.gov/pubmed/24172896) *Nature*. 2013;503(7475):277-80.

2. Gautam R, Nishimura Y, Pegu A, Nason MC, Klein F, Gazumyan A, Golijanin J, Buckler-White A, Sadjadpour R, Wang K, Mankoff Z, Schmidt SD, Lifson JD, Mascola JR, Nussenzweig MC, Martin MA. A single injection of anti-HIV-1

antibodies protects against repeated SHIV challenges. (https://www.ncbi.nlm.nih.gov/pubmed/27120156) *Nature*. 2016;533(7601):105-109.

3. Nishimura Y, Gautam R, Chun TW, Sadjadpour R, Foulds KE, Shingai M, Klein F, Gazumyan A, Golijanin J, Donaldson M, Donau OK, Plishka RJ, Buckler-White A, Seaman MS, Lifson JD, Koup RA, Fauci AS, Nussenzweig MC, Martin MA. Early antibody therapy can induce long-lasting immunity to SHIV. (https://www.ncbi.nlm.nih.gov/pubmed/28289286) *Nature*. 2017;543(7646):559-563.

4. Gautam R, Nishimura Y, Gaughan N, Gazumyan A, Schoofs T, Buckler-White A, Seaman MS, Swihart BJ, Follmann DA, Nussenzweig MC, Martin MA. A single injection of crystallizable fragment domain-modified antibodies elicits durable protection from SHIV infection. (https://www.ncbi.nlm.nih.gov/pubmed/29662199) *Nat Med*. 2018;24(5):610-616.

5. Escolano A, Gristick HB, Abernathy ME, Merkenschlager J, Gautam R, Oliveira TY, Pai J, West AP Jr, Barnes CO, Cohen AA, Wang H, Golijanin J, Yost D, Keeffe JR, Wang Z, Zhao P, Yao KH, Bauer J, Nogueira L, Gao H, Voll AV, Montefiori DC, Seaman MS, Gazumyan A, Silva M, McGuire AT, Stamatatos L, Irvine DJ, Wells L, Martin MA, Bjorkman PJ, Nussenzweig MC. Immunization expands B cells specific to HIV-1 V3 glycan in mice and macaques. (https://www.ncbi.nlm.nih.gov/pubmed/31142836) *Nature*. 2019;570(7762):468-473.

Related Scientific Focus Areas

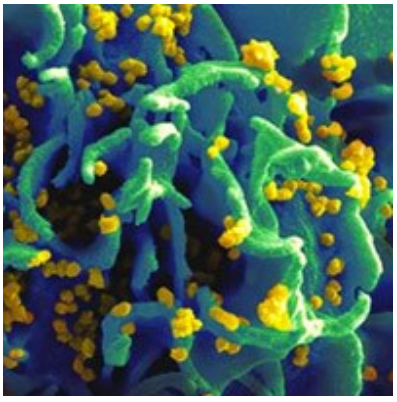

Virology

View additional Principal Investigators in Virology (https://irp.nih.gov/our-research/principal-investigators/focus/virology)

LEARN MORE (https://irp.nih.gov/our-research/scientific-focus-areas/virology)

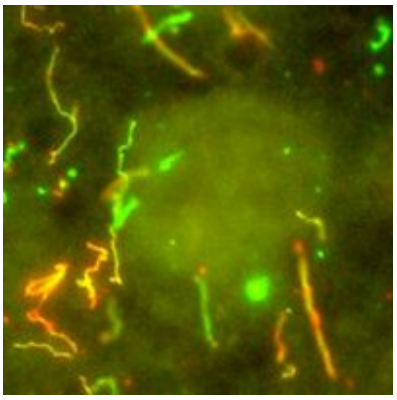

Microbiology and Infectious Diseases

View additional Principal Investigators in Microbiology and Infectious Diseases (https://irp.nih.gov/our-research/principal-investigators/focus/microbiology-and-infectious-diseases)

LEARN MORE (https://irp.nih.gov/our-research/scientific-focus-areas/microbiology-and-infectious-diseases)

Molecular Biology and Biochemistry

View additional Principal Investigators in Molecular Biology and Biochemistry (https://irp.nih.gov/our-research/principal-investigators/focus/molecular-biology-and-biochemistry)

LEARN MORE (https://irp.nih.gov/our-research/scientific-focus-areas/molecular-biology-and-biochemistry)

This page was last updated on August 9th, 2019

JOURNAL OF VIROLOGY, Aug. 1986, p. 284–291
0022-538X/86/080284-08$02.00/0

Vol. 59, No. 2

Production of Acquired Immunodeficiency Syndrome-Associated Retrovirus in Human and Nonhuman Cells Transfected with an Infectious Molecular Clone

AKIO ADACHI,[1]* HOWARD E. GENDELMAN,[1] SCOTT KOENIG,[2] THOMAS FOLKS,[2] RONALD WILLEY,[1] ARNOLD RABSON,[1] AND MALCOLM A. MARTIN[1]

Laboratory of Molecular Microbiology[1] *and Laboratory of Immunoregulation,*[2] *National Institute of Allergy and Infectious Diseases, National Institutes of Health, Bethesda, Maryland 20892*

Received 3 March 1986/Accepted 15 April 1986

We constructed an infectious molecular clone of acquired immunodeficiency syndrome-associated retrovirus. Upon transfection, this clone directed the production of infectious virus particles in a wide variety of cells in addition to human T4 cells. The progeny, infectious virions, were synthesized in mouse, mink, monkey, and several human non-T cell lines, indicating the absence of any intracellular obstacle to viral RNA or protein production or assembly. During the course of these studies, a human colon carcinoma cell line, exquisitely sensitive to DNA transfection, was identified.

A group of T-lymphotropic retroviruses (RVs), with a genomic structure characteristic of lentiviruses (34), has been isolated from patients with acquired immunodeficiency syndrome (AIDS), AIDS-related complex, and generalized lymphadenopathy (2, 9, 23). During its propagation in vitro, the virus selectively infects and ultimately kills the subset of human T lymphocytes exhibiting the OKT4-Leu-3 phenotype (7, 20), the same cells that are profoundly affected in individuals suffering from the disease (14, 15).

Mechanisms responsible for cell- and species-specific tropism(s) have been studied in a number of retroviral systems. For both avian and murine RVs, restriction affecting the interaction of the viral envelope glycoprotein and a specific cell receptor has been demonstrated repeatedly and is responsible for the unique host range of xenotropic and ecotropic mouse leukemia viruses (for a review, see reference 36). In the murine system, at least, retroviral restriction or tropism may also be determined at a point subsequent to adsorption and penetration. For example, the thymotropism exhibited by many mink cell focus-forming murine leukemia viruses very likely reflects the properties of enhancer elements present within the long terminal repeats of these recombinant murine leukemia viruses (5). Furthermore, *Fv-1* (29) restriction involves the interaction of viral capsid proteins (18, 19, 31) and certain cell component(s) during the early phase of infection.

In this report, the potential restriction of AIDS RV replication in non-T4 lymphocytes was evaluated. Because the transfection of an infectious molecular clone of the AIDS RV provirus would bypass any barrier imposed by the interaction of virus particles with their receptors, intracellular restriction affecting the expression of viral genes can be readily examined. Cloned AIDS RV DNA was introduced into 3 human lymphoid, 11 human nonlymphoid, and 3 nonhuman cell lines. The progeny, infectious virions, were detected in 14 of the 17 transfected cell lines, indicating the absence of any intracellular obstacle to viral RNA or protein synthesis and assembly.

* Corresponding author.

MATERIALS AND METHODS

Cells. The cell lines used in these studies are listed in Table 1. The three human lymphoid cell lines were propagated and maintained in RPMI 1640 medium supplemented with heat-inactivated (56°C for 30 min) 10% fetal calf serum. The adherent cell lines listed in Table 1 were cultured in Dulbecco modified Eagle minimal essential medium containing heat-inactivated 10% fetal calf serum. Normal human peripheral blood lymphocytes (PBLs) were cryopreserved and stored in liquid nitrogen until needed. Before use, the PBLs were quickly thawed, washed, and prepared for infection as described previously (2).

Construction of an infectious molecular clone. The origin of the NY5 and LAV AIDS RV isolates has been outlined previously (2, 3). Molecular clones of integrated NY5 and LAV proviruses were obtained from bacteriophage lambda DNA libraries constructed from *Eco*RI-restricted preparations of virus-infected PBLs. NY5 proviral DNA, like other North American isolates, contained a single *Eco*RI site at 5.7 kilobases (kb) and was cloned as two separate restriction fragments containing either 5′ or 3′ flanking cellular DNA. Integrated NY5 proviruses, cloned in *Eco*RI-digested λ Charon 4A (4), were identified by hybridization to ^{32}P-labeled pBenn6, which contains 6.5-kb AIDS RV sequences mapping between 1.7 and 8.2 kb (8). Molecular clones containing sequences located 3′ to the *Eco*RI site at 5.7 kb of LAV proviral DNA were isolated from a λJ1 (28) library after hybridization with ^{32}P-labeled pBenn4 (8). The cloned NY5 and LAV proviruses were then transferred to *Eco*RI-digested pUC18 and subsequently used to construct full-length clones.

Transfection assays. Nonlymphoid and lymphoid cells were transfected by the calcium phosphate precipitation (16, 37) and electroporation (30) techniques, respectively, with 10 μg of uncleaved plasmid DNA in each assay. Virus production was monitored in non-T4 cells by cocultivation with CD4$^+$ A3.01 cells (10^6 cells of each type) 2 days after transfection. Reverse transcriptase (RT) assays were carried

TABLE 1. Cell lines used for transfection

Cell line	Description	Virus production[a]		Source or reference
		Co-culture	Filtrate	
A3.01	Human T-cell leukemia	+	+	8
BJAB	Human B-cell lymphoma (EBV−)[b]	+	ND	22
Raji	Human B-cell lymphoma (EBV+)[c]	−	ND	ATCC CCL86
A-204	Human rhabdomyosarcoma cells	+	+	ATCC HTB82
CHP126	Human neuroblastoma cells	−	ND	1
HMB2	Human melanoma cells	+	ND	39
CAPAN-1	Human pancreatic carcinoma cells	+	+	ATCC HTB79
SK-OV-3	Human ovarian carcinoma cells	+	+	ATCC HTB77
T47D	Human breast carcinoma cells	−	ND	39
CaCO-2	Human colon carcinoma cells	+	+	ATCC HTB37
SK-CO-1	Human colon carcinoma cells	+	ND	ATCC HTB39
HT-29	Human colon carcinoma cells	ND	+	ATCC HTB38
SW480	Human colon carcinoma cells	ND	+	ATCC CCL228
SW1463	Human rectal carcinoma cells	ND	+	ATCC CCL234
Mink	Mink lung epithelial cells	+	ND	ATCC CCL64
COS-1	Monkey kidney cells transformed by simian virus 40	+	+	12
NIH 3T3	Mouse fibroblast cells	+	ND	ATCC CCL92

[a] +, Production; −, no production. ND, Not determined.
[b] EBV−, Epstein-Barr virus negative.
[c] EBV+, Epstein-Barr virus positive.

out at various times after cocultivation as described previously (8).

In situ hybridization. Transfected cell preparations were sedimented onto polylysine-coated glass slides, fixed in periodate-lysine-paraformaldehyde-glutaraldehyde, and pretreated with HCl and proteinase K to allow the labeled probe to enter the cells (10, 11). Cells were prehybridized in 10 mM Tris (pH 7.4)–2× standard saline citrate (SSC) (1× SSC is 0.15 M NaCl plus 0.015 M sodium citrate [pH 7.4])–50% formamide–1× Denhardt solution (0.02% polyvinylpyrrolidone, 0.02% Ficoll [Pharmacia Fine Chemicals, Piscataway, N.J.], 0.02% bovine serum albumin)–200 μg of yeast tRNA per ml at 45°C for 2 h and were hybridized in this solution plus 10% dextran sulfate, 5 μM dithiothreitol, and 10^6 cpm of ^{35}S-labeled AIDS RV RNA in 10-μl reaction mixtures. Subgenomic viral DNA fragments present in pB1 (3), pBenn6 (8), pB11 (3), and a recombinant plasmid (pRG-B) which contains a 1.35-kb *Hin*dIII fragment mapping between 8.25 and 9.6 kb on the proviral DNA were subcloned into SP6/T7 vectors (Promega Biotec, Madison, Wis.), and the pooled DNAs were transcribed with ^{35}S-labeled UTP (Amersham Corp., Arlington Heights, Ill.). The labeled RNAs were incubated with 40 μM $NaHCO_3$–60 μM Na_2CO_3 [pH 10.2] before hybridization to facilitate their entry into cells.

Hybridization was performed at 45°C for 8 h. The samples were then washed in 2× SSC at 22°C for 10 min, with two changes; 2× SSC–0.1% Triton X-100 at 60°C for 30 min; 2× SSC plus RNase A (40 μg/ml) and RNase T_1 (10 U/ml) at 37°C for 30 min; and 2× SSC at 60°C for 10 min. All solutions except those with RNase A contained 5 μM dithiothreitol and 1 μM EDTA. Autoradiography was performed for 1 to 2 days as described previously (11).

CAT assays. Chloramphenicol acetyltransferase (CAT) assays with pSV2CAT DNA have been described previously (13). The uptake of pSV2CAT DNA into transfected cells was monitored by dot blot hybridization using ^{32}P-labeled pUC18 DNA.

RESULTS

Construction of full-length clones of the AIDS RV provirus. Our previous experience indicated that only a minority of cloned murine leukemia virus proviral DNAs were infectious after their introduction into susceptible cells. Therefore, we decided to take advantage of the single *Eco*RI site that virtually bisected (located at 5.7 kb) the proviruses of North American AIDS RV isolates (3), and we elected to mix and match 5′ and 3′ halves of integrated proviral DNAs that had been obtained from different infected cellular DNA libraries. Representative examples are shown in the top portion of Fig. 1. λN5′ consisted of a 20.2-kb *Eco*RI fragment in λ Charon 4A that was cloned from a library of NY5-infected PBLs. λL3 and λL4 were isolated from LAV-infected cellular DNA preparations with a 3′ AIDS RV probe and consisted of 7.5- and 13.6-kb *Eco*RI inserts, respectively, in a λJ1 phage vector. An 8.3-kb *Bam*HI-*Eco*RI subclone of λN5′ was introduced into *Bam*HI-*Eco*RI-digested pUC18 to generate a plasmid designated pN5′. Because pN5′ contained a single *Eco*RI site, *Eco*RI fragments containing the 3′ half of the AIDS RV provirus could be readily introduced, thereby generating full-length and potentially infectious constructs. The *Eco*RI segments from λL3 (both orientations) and λL4 were inserted into pN5′ (Fig. 1). Of note is the presence of a unique *Hin*cIII site at 8.7 kb in pNL4-3; a *Hin*cII site at this position (representing a restriction enzyme site polymorphism in the parental LAV virus stock) had been previously identified in an isolate from Alabama (3).

Infectivity of full-length AIDS RV proviral DNA constructs was monitored after electroporation into A3.01 cells. We have previously reported that the A3.01 cell line is >95% Leu-3$^+$ Leu-8$^+$ Leu-1$^+$ and is exquisitely sensitive to AIDS RV infection, exhibiting the same viral cytopathic effect observed in infected PBLs, including cell death (8). Only the pNL4-3 DNA construct was infectious after its introduction into A3.01 cells (Fig. 2). Syncytia were visualized in cultures transfected with pNL4-3 DNA as early as day 9. This was followed by a peak of RT activity on day 16, as well as by a profound reduction in the number of viable cells. pNL3-2 DNA failed to elicit any cytopathic effect or RT activity after its electroporation into A3.01 cells. Because pNL3-2 contained the same 5′ 5.7 kb of AIDS RV sequences present in the infectious plasmid pNL4-3, an alteration affecting viral sequences mapping 3′ to the *Eco*RI joint most likely explains the loss of biological activity.

Transfection of the infectious molecular clone of the AIDS RV into nonhuman T cells. Viral infectivity studies indicate that, with few exceptions (24, 27), the AIDS RV can only be propagated in the Leu-3-OKT4 helper-inducer subset of human T lymphocytes. This selective cell tropism most likely reflects the interaction of AIDS RV particles with a

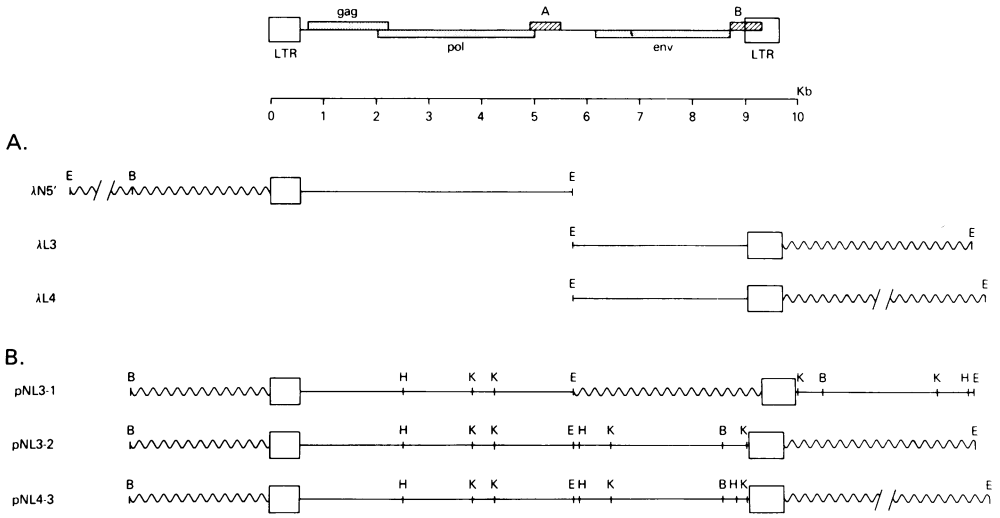

FIG. 1. Construction of full-length clones of AIDS RV. Integrated NY5 and LAV proviruses were cloned in λ Charon 4A (λN5′) or λJ1 (λL3 and λL4), respectively (A). The *Eco*RI inserts of λL3 (both orientations) and λL4 were introduced into the *Eco*RI site of plasmid pN5′ DNA, which contained the *Bam*HI-*Eco*RI segment from λN5′ (see Materials and Methods) (B). Only inserts are shown. A schematic diagram of AIDS proviral DNA is shown at the top of the figure. Abbreviations: B, *Bam*HI; E, *Eco*RI; H, *Hin*cII; K, *Kpn*I.

specific receptor(s) (7, 21, 26) on the surface of CD4$^+$ lymphocytes. However, intracellular restriction involving, for example, the activity of viral promoter or enhancer or the assembly of viral proteins and genomic RNA into infectious virions has not been formally ruled out. The existence of such an intracellular block could readily be evaluated with an infectious clone of the AIDS provirus, since the barrier imposed by a specific cell receptor would no longer be a factor.

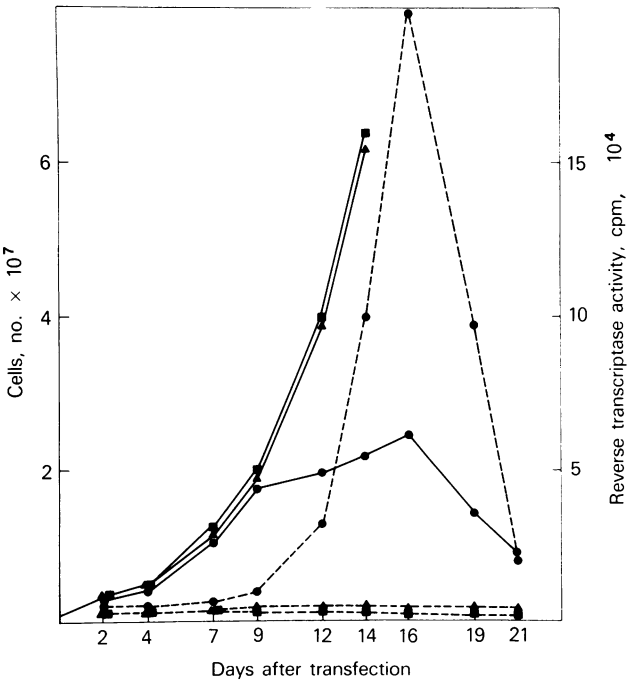

FIG. 2. Kinetics of virus infection after transfection of A3.01 cells. On day 0, pNL4-3 (●), pNL3-2 (▲), or pNL3-1 (■) was introduced into A3.01 cells by electroporation, and 10^6 viable cells were placed in culture. The number of viable cells in the culture (——) and RT activity (– – –) were monitored on the days indicated.

pNL4-3 DNA was introduced into the 16 non-T cell lines listed in Table 1, which included both human and nonhuman cells. Because none of these transfected cells would be expected to express the putative receptor for the AIDS RV, it seemed very unlikely that progeny, virus particles produced as a result of the initial transfection, would reinfect other cells in the culture. Because insufficient numbers of virions would be generated to be detected directly by the RT assay, CD4$^+$ A3.01 cells were added to the cultures 48 h after transfection to amplify any virions that appeared. The presence of virus was monitored by RT assays at various times after cocultivation. Of the 16 non-T cell lines, 13 yielded infectious AIDS RV particles as a consequence of transfection with pNL4-3 DNA (Fig. 3 and Table 1). In most cases, the peak of RT activity was detected 14 to 16 days after transfection (12 to 14 days after cocultivation with A3.01 cells); cocultures of COS-1 (monkey) and SK-OV-3 (human ovarian carcinoma) cells exhibited more rapid kinetics of virus production. A repeat of the experiment depicted in Fig. 3 gave similar results. In a parallel experiment that omitted cocultivation with A3.01 cells, no RT was detected. To rule out the possibility that the non-T cell lines might harbor a cryptic lymphotropic virus with RT activity, each was cocultivated with A3.01 cells for 4 weeks; no infectious virus was detected. In addition, when the noninfectious molecular clone of the AIDS RV, pNL3-1, was transfected into each of the cell lines listed in Table 1, no infectious virions were generated, even after 4 weeks of coculture.

We were interested in ascertaining whether the progeny, virus particles synthesized in non-T cells, entered A3.01 cells by cell-to-cell transfer or whether they budded into the tissue culture medium and subsequently adsorbed to viral receptors on the CD4$^+$ target cells. Cell-free supernatants obtained from eight (A204, CAPAN-1, CaCO-2, HT-29, SK-OV-3, SW480, SW1463, COS-1) of the cell lines 48 h after transfection and prepared by filtration of tissue culture medium through 0.45-μm-pore membranes were used to infect phytohemagglutinin-stimulated PBLs. Infectious AIDS RV was present in all of the supernatants tested, with

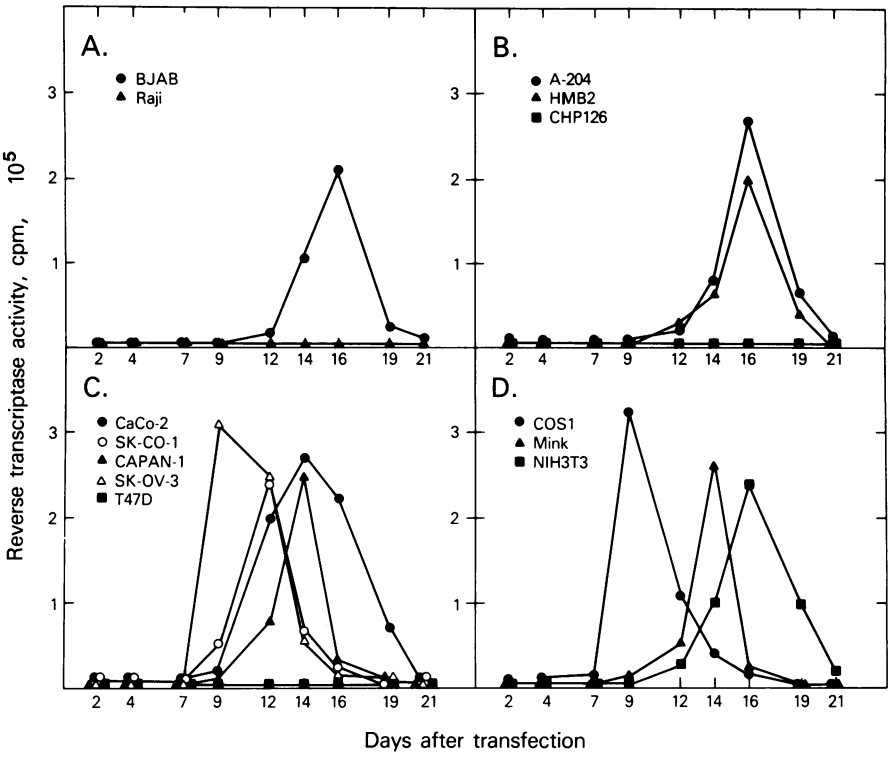

FIG. 3. Kinetics of RT activity in transfected cells cocultivated with A3.01 cells. On day 2 after transfection with the infectious molecular clone pNL4-3, 10^6 cells were cocultured with 10^6 A3.01 cells, and RT activity was monitored on the days indicated. See Table 1 for the description of each cell line.

peaks of RT detected 5 to 14 days after infection of the PBLs (Table 1). No virus was detected when the supernatants of mock-infected cultures were examined.

Replication of the AIDS RV in non-T cells was also monitored by in situ hybridization. Viral RNA was readily detected in the A204 rhabdomyosarcoma cell line 2 days after transfection (Fig. 4A). RNase treatment of the transfected cell preparation before hybridization reduced the signal to background levels (zero to two grains per cell). Assuming that five grains above background (seven or more grains per cell) indicated the presence of AIDS RV RNA, approximately 6.7% of the A204 cells were synthesizing viral RNA 48 h after transfection. The number of cells expressing viral RNA fell precipitously thereafter, to 0.2% on day 3 and to 0 (out of 10^5 A204 cells examined) on day 7. The recovery of virus by cocultivation with A3.01 cells on days 2 and 3 but not on day 7 (data not shown) is consistent with these in situ hybridization results. Similar transient expression of AIDS RV RNA was observed in BJAB, SW480, and NIH 3T3 cells transfected with pNL4-3 DNA (data not shown).

Failure to obtain a chronic AIDS RV-producing line. Because the non-T cell lines listed in Table 1, which synthesized infectious virus particles after transfection, apparently lacked the receptor(s) that would permit the initial burst of virions to spread throughout the culture, the possibility existed that cells continuously producing virus might be isolated from the mass culture of the transfected cells. Therefore, A204 cells were cotransfected with pSV2NEO and pNL4-3 DNAs (in a molar ratio of 1:10, respectively), and G418-resistant cells were selected as described previously (35). In a companion experiment, no G418-resistant clones were obtained from mock-transfected cells. None of the 92 G418-resistant cell clones that were isolated during a 3-week period synthesized infectious AIDS RV after cocultivation with A3.01 cells. This result suggested that the resistant A204 cells, although containing the pSV2NEO gene, harbored either a defective copy or no proviral DNA. This finding also raised the possibility that nonlymphoid cells undergoing productive infection with the AIDS virus may also be killed in the process.

Identification of a human cell line that is exquisitely sensitive to transfection by cloned AIDS RV proviral DNA. During the examination of cell-free filtrates obtained from nonlymphoid cells transfected with the infectious clone of the AIDS provirus, we observed that one of the supernatants contained high levels of RT activity. A more careful evaluation of the human colon carcinoma cell line SW480 revealed that substantial amounts of RT activity were detectable 24 h posttransfection (Fig. 5); these levels gradually fell to background levels over a 3-week period. When the experiment depicted in Fig. 5 was monitored by in situ hybridization, 25 and 19% of the transfected SW480 cells were found to be synthesizing viral RNA on days 1 and 2, respectively (Fig. 4B). In comparison with a cloned human $CD4^+$ lymphocyte cell line (S. Koenig, unpublished data) productively infected with the AIDS RV (Fig. 4D), SW480 cells, expressing viral gene products, contained two to five times more grains.

We considered the possibility that the unique susceptibility of SW480 cells to cloned AIDS RV proviral DNA might represent a more global sensitivity to DNA transfection. Therefore, pSV2CAT DNA was introduced into the seven cell lines indicated in Table 2; conversion of chloramphenicol to its acetylated form, as well as DNA uptake, was measured in each case. When normalized for DNA uptake, SW480 cells were at least five times more efficient in CAT gene expression than any of the other cells lines examined.

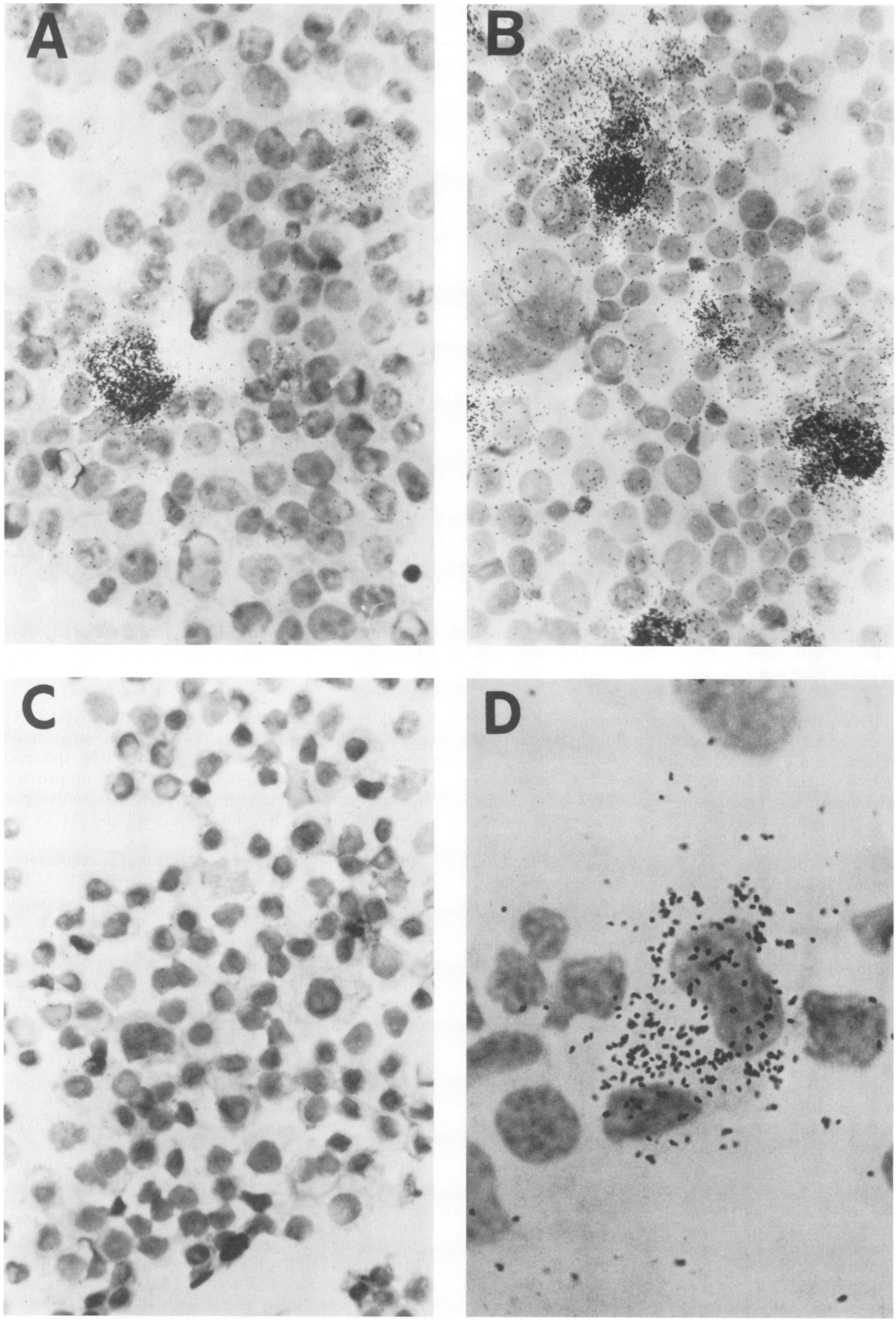

FIG. 4. In situ hybridization of cells transfected with the infectious molecular clone of the AIDS RV. A-204 (A) and SW480 (B) cells were subjected to in situ hybridization 48 h after transfection with pNL4-3 DNA. Mock-transfected A-204 (C) and LAV-infected $CD4^+$ lymphocyte (D) cells are also shown. Magnification in panels A, B, and C, ×100; magnification in panel D, ×400.

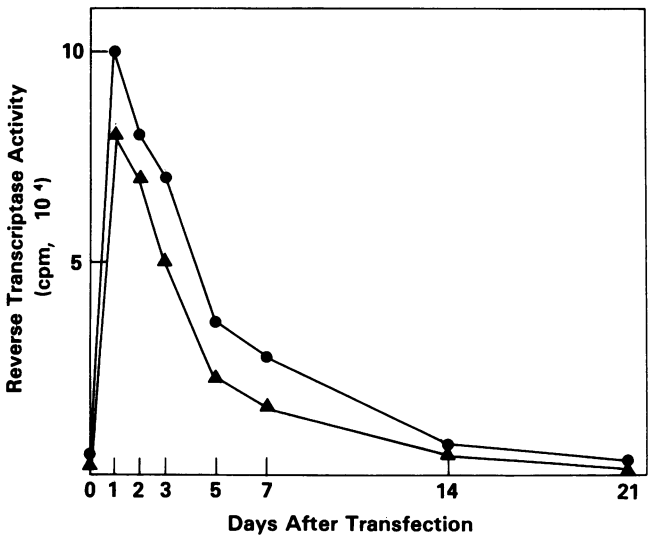

FIG. 5. Kinetics of RT activity in SW480 cells transfected with the infectious clone pNL4-3. On day 0, 3×10^6 SW480 cells were transfected with the infectious clone pNL4-3 by the calcium phosphate precipitation method, and RT activity in the tissue culture medium was monitored on the days indicated. ● and ▲ indicate the results of two independent experiments.

DISCUSSION

A major conclusion of our experiments involving the transfection of an infectious molecular clone of the AIDS virus into several different cell lines is that the interaction of AIDS RV particles with their receptor(s) is clearly the principal determinant of cell tropism. Once this cell surface restriction is negotiated, viral RNA and proteins are synthesized and assembled into infectious and cytopathic virions, irrespective of cell type. Although this result might have been inferred from earlier studies which showed that the AIDS RV-*trans*-activating determinant functioned in a variety of cell types (33), this is the first report to demonstrate that non-T cells of four different mammalian species are capable of generating infectious virus.

Unlike the situation with the cloned provirus of HTLV-II, which required cotransfection and selection with G418 (6), infectivity with pNL4-3 DNA was observed after its introduction into the $CD4^+$ A3.01 cells without the use of selective pressure. A characteristic feature of transfecting non-T cells with the cloned AIDS RV provirus is the relatively short period (usually up to 7 days) during which progeny are synthesized. This transient production of virions, shown graphically in Fig. 5, most likely reflects the failure of the input DNA to stably integrate into the chromosome of the transfected cells. Concatemers of the cloned viral DNA formed during calcium phosphate precipitation (16, 37) may function as pseudointegrated templates for AIDS RV RNA synthesis for relatively brief periods of time, after which they are degraded or otherwise eliminated. Another explanation for the transient expression of virus production after transfection is that cells are killed as a consequence of synthesizing and assembling viral gene products. Proving cell death after the introduction of viral DNA in the systems we used is technically very difficult. At best, about 20% of transfected cells (in the case of SW480) were synthesizing viral RNA during the first 48 h after transfection. Unlike experiments with $CD4^+$ lymphocytes in which virtually all of the cells are killed by waves of newly synthesized virions, nonlymphocytes, dying as a result of a productive virus infection, would be replaced in the monolayer by neighboring cells lacking the receptor(s) for secondary infection by the progeny, AIDS RV particles, and would thereby escape detection. Furthermore, the failure to obtain G418-resistant cells that produce infectious viral particles after cotransfection with pSV2NEO and pNL4-3 DNAs is certainly consistent with the death of nonlymphocytes expressing AIDS RV gene products.

Transfection of the cloned AIDS RV provirus resulted in virus production in 13 of the 16 non-T cells examined. The three instances in which no virus was detected should not be presently viewed as examples of intracellular restriction. Although no virus was generated after the introduction of the infectious clone into Raji cells, a second B-lymphocyte line (BJAB) synthesized replication-competent virions (Table 1). Factors associated with the transfection assay per se, such as the efficiency of DNA uptake, could very likely be responsible for the failure to detect virus particles in all of the cell lines examined.

A by-product of these investigations was the discovery of a human colon carcinoma cell line that was particularly sensitive to transfection. AIDS RV virions were demonstrable in cultures of SW480 cells 24 h posttransfection, thereby obviating the necessity for cocultivation with $CD4^+$ target cells. This susceptibility to transfection also extended to non-RV DNAs in experiments involving pSV2CAT DNA. At the present time, we have no explanation for this unique property of SW480 cells. Certainly, the augmented expression of transfected DNA is not due to increased DNA uptake (Table 2), nor is it a characteristic feature of colon carcinoma cells, since four other cell lines (Table 1) failed to exhibit this property of SW480 cells.

We (3) and others (17, 25, 32, 38) have noted that the genomic heterogeneity of the AIDS RV genome affects primarily *env* gene sequences. Because the studies described in this report demonstrate that the main determinant of cell tropism involves the interaction of the viral envelope and cell receptor(s), it is tempting, from an evolutionary viewpoint, to link *env* variability to the appearance of the AIDS virus as a human pathogen. Stripped of its capsid and envelope proteins, the cloned viral DNA was expressed as

TABLE 2. Relative CAT activity in cells transfected with pSV2CAT

Cell line	Description	% Conversion[a]	DNA uptake[b]	CAT activity[c]
SW480	Human colon cells	83.0	1.0	100
SK-CO-1	Human colon cells	6.8	1.2	7
SK-OV-3	Human ovarian cells	33.8	2.0	20
CAPAN-1	Human pancreatic cells	10.2	0.7	18
A-204	Human rhabdomyosarcoma cells	3.2	1.1	4
HMB2	Human melanoma cells	0.5	0.2	3
NIH 3T3	Mouse fibroblasts	0.7	0.8	1

[a] CAT assays were done with equivalent amounts of protein from each cell lysate (100 μg per assay). After analysis by ascending thin-layer chromotography, the rates of conversion were determined by scintillation counting. CAT activity of mock-transfected cell lysates was less than 0.1%.

[b] DNA uptake was determined by dot blot hybridization using ^{32}P-labeled pUC18 DNA. Membranes were subsequently monitored in a liquid scintillation counter, and DNA uptake was normalized relative to that of SW480 cells. The counts hybridized per minute varied from 2,338 (HMB2) to 29,700 (SK-OV-3); mock-transfected cultures contained less than 200 cpm.

[c] CAT activity was normalized for conversion and DNA uptake relative to that of SW480 cells.

infectious virus in virtually all cells tested. One could propose that an alteration more profound than is normally observed in the *env* region of different AIDS RV isolates drastically alters the cell and species target of a progenitor to the AIDS virus. In the process, such a virus could lose its original tropism and assume a new ecological niche: the helper and inducer $CD4^+$ lymphocytes of humans.

ACKNOWLEDGMENTS

We thank B. Johnson for RT assays, T. Bryan for λ cloning, and S. Rosenfeld for typing the manuscript.

LITERATURE CITED

1. **Balaban-Malenbaum, G., and F. Gilbert.** 1977. Double minute chromosomes and the homogeneously staining regions in chromosomes of a human neuroblastoma cell line. Science **198**:739–741.
2. **Barre-Sinoussi, F., J. C. Cherman, R. Rey, M. T. Nugeryre, S. Chamaret, J. Gruest, C. Dauget, C. Axler-Blin, F. Vezinet-Brun, C. Rouzioux, W. Rosenbaum, and L. Montagnier.** 1983. Isolation of a T-lymphotrophic retrovirus from a patient at risk for acquired immune deficiency syndrome (AIDS). Science **220**: 868–871.
3. **Benn, S., R. Rutledge, T. Folks, J. Gold, L. Baker, J. McCormic, P. Feorino, P. Piot, T. Quinn, and M. Martin.** 1985. Genomic heterogeneity of AIDS retroviral isolates from North America and Zaire. Science **230**:949–951.
4. **Blattner, F. R., G. Williams, A. E. Blechl, K. Denniston-Thompson, H. E. Farber, L. Furlong, D. J. Grunwald, D. O. Kiefer, D. D. Moore, J. W. Schumm, E. L. Sheldon, and O. Smithies.** 1979. Charon phages: safer derivatives of bacteriophage λ for DNA cloning. Science **196**:161–169.
5. **Celander, D., and W. A. Haseltine.** 1984. Tissue-specific transcription preference as a determinant of cell tropism and leukaemogenic potential of murine retroviruses. Nature (London) **312**:159–162.
6. **Chen, I. S. Y., J. McLaughlin, and D. W. Golde.** 1984. Long terminal repeats of human T-cell leukemia virus II genome determine target cell specificity. Nature (London) **309**:276–279.
7. **Dalgleish, A. G., P. C. L. Beverley, P. R. Clapham, D. H. Crawford, M. F. Greaves, and R. A. Weiss.** 1984. The CD4(T4) antigen is an essential component of the receptor for the AIDS retrovirus. Nature (London) **312**:763–767.
8. **Folks, T., S. Benn, A. Rabson, T. Theodore, M. D. Hoggan, M. Martin, M. Lightfoote, and K. Sell.** 1985. Characterization of a continuous T-cell line susceptible to the cytopathic effects of the acquired immunodeficiency syndrome (AIDS)-associated retrovirus. Proc. Natl. Acad. Sci. USA **82**:4539–4543.
9. **Gallo, R. C., S. Z. Salahuddin, M. Popovic, G. M. Shearer, M. Kaplan, B. F. Haynes, T. J. Palker, R. Redfield, J. Oleske, B. Safai, G. White, P. Foster, and P. D. Markham.** 1984. Frequent detection and isolation of cytopathic retroviruses (HTLV-III) from patients with AIDS and at risk for AIDS. Science **224**:500–503.
10. **Gendelman, H. E., T. R. Moench, O. Narayan, and D. E. Griffin.** 1983. Selection of a fixative for identifying T cell subsets, B cells, and macrophages in paraffin-embedded mouse spleen. J. Immunol. Methods **65**:137–145.
11. **Gendelman, H. E., O. Narayan, S. Molineaux, J. E. Clements, and Z. Ghotbi.** 1985. Slow, persistent replication of lentiviruses: role of tissue macrophages and macrophage precursors in bone marrow. Proc. Natl. Acad. Sci. USA **82**:7086–7090.
12. **Gluzman, Y.** 1981. SV40-transformed simian cells support the replication of early SV40 mutants. Cell **23**:175–182.
13. **Gorman, C. M., L. F. Moffat, and B. H. Howard.** 1982. Recombinant genomes which express chloramphenicol acetyltransferase in mammalian cells. Mol. Cell. Biol. **2**:1044–1051.
14. **Gottlieb, M. S., J. E. Groopman, W. M. Weinstein, J. L. Fahey, and R. Detels.** 1983. The acquired immunodeficiency syndrome. Ann. Intern. Med. **99**:208–220.
15. **Gottlieb, M. S., R. Schroff, H. M. Schanker, J. D. Weisman, P. T. Fan, R. A. Wolf, and A. Saxon.** 1981. *Pneumocystis carinii* pneumonia and mucosal candidiasis in previously healthy homosexual men: evidence of a new acquired cellular immunodeficiency. N. Engl. J. Med. **305**:1425–1431.
16. **Graham, F. L., and A. J. Van der Eb.** 1973. A new technique for the assay of infectivity of human adenovirus 5 DNA. Virology **52**:456–467.
17. **Hahn, B. H., M. A. Gonda, G. M. Shaw, M. Popovic, J. A. Hoxie, R. C. Gallo, and F. Wong-Staal.** 1985. Genomic diversity of the acquired immune deficiency syndrome virus HTLV-III: different viruses exhibit greatest divergence in their envelope genes. Proc. Natl. Acad. Sci. USA **82**:4813–4817.
18. **Hopkins, N., J. Schindler, and P. D. Gottlieb.** 1977. Evidence for recombination between N- and B-tropic murine leukemia viruses. J. Virol. **21**:1074–1078.
19. **Hopkins, N., J. Schindler, and R. Hynes.** 1977. Six NB-tropic murine leukemia viruses derived from a B-tropic virus of BALB/c have altered p30. J. Virol. **21**:309–318.
20. **Klatzmann, D., F. Barre-Sinoussi, M. T. Nugeryre, C. Daugnet, E. Vilmer, C. Griscelli, F. Brun-Vezinet, C. Rouzioux, J. C. Gluckman, J. C. Chermann, and L. Montagnier.** 1984. Selective tropism of lymphadenopathy associated virus (LAV) for helper-inducer T-lymphocytes. Science **255**:59–63.
21. **Klatzman, D., E. Champagne, S. Chamaret, J. Gruest, D. Guetard, T. Hercend, J. C. Gluckmann, and L. Montagnier.** 1984. T-lymphocyte T4 molecule behaves as the receptor for human retrovirus LAV. Nature (London) **312**:767–770.
22. **Klein, G., T. Lindahl, M. Jondal, W. Leibold, J. Menezes, K. Nilsson, and C. Sundstrome.** 1974. Continuous lymphoid cell lines with B-cell characteristics that lack the Epstein-Barr virus genome, derived from three human lymphomas. Proc. Natl. Acad. Sci. USA **71**:3283–3286.
23. **Levy, J. A., A. D. Hoffman, S. M. Kramer, J. A. Lanois, J. M. Shimabukuro, and L. S. Oskiro.** 1984. Isolation of lymphocytopathic retroviruses from San Francisco patients with AIDS. Science **225**:840–842.
24. **Levy, J. A., J. Shimabukuro, T. McHugh, C. Casavant, D. Stites, and L. Oshiro.** 1985. AIDS-associated retroviruses (ARV) can productively infect other cells besides human T helper cells. Virology **147**:441–448.
25. **Luciw, P. A., S. J. Potter, K. Steimer, D. Dina, and J. A. Levy.** 1984. Molecular cloning of AIDS-associated retrovirus. Nature (London) **312**:760–763.
26. **McDougal, J. S., M. S. Kennedy, J. N. Sligh, S. P. Cort, A. Mawle, and J. K. A. Nicholson.** 1985. Binding of HTLV-III/LAV to $T4^+$ T cells by a complex of the 110K viral protein and the T4 molecule. Science **231**:382–385.
27. **Montagnier, L., J. Gruest, S. Chamaret, C. Dauguet, C. Axler, C. Guetard, M. T. Nugeryre, F. Barre-Sinoussi, J. C. Chermann, J. B. Brunt, D. Klatzman, and J. C. Gluckman.** 1984. Adaptation of lymphadenopathy-associated virus (LAV) to replication in EBV-transformed B lymphoblastoid cell lines. Science **225**:63–66.
28. **Mullins, J. I., D. S. Brody, R. C. Binari, Jr., and S. M. Cotter.** 1984. Viral transduction of c-*myc* gene in naturally occurring feline leukaemias. Nature (London) **308**:856–858.
29. **Pincus,T., J. W. Hartley, and W. P. Rowe.** 1971. A major genetic locus affecting resistance to infection with murine leukemia viruses. I. Tissue culture studies of naturally occurring viruses. J. Exp. Med. **133**:1219–1223.
30. **Potter, H., W. Lawrence, and P. Leder.** 1984. Enhancer-dependent expression of human K immunoglobulin genes introduced into mouse pre-B lymphocytes by electroporation. Proc. Natl. Acad. Sci. USA **81**:7161–7165.
31. **Schlindler, J., R. Hynes, and N. Hopkins.** 1977. Evidence for recombination between N- and B-tropic murine leukemia viruses: analysis of three virion proteins by sodium dodecyl sulfate-polyacrylamide gel electrophoresis. J. Virol. **23**:700–707.
32. **Shaw, G. M., B. H. Hahn, S. K. Arya, J. E. Groupmann, R. C. Gallo, and F. Wong-Staal.** 1984. Molecular characterization of human T-cell leukemia (lymphotropic) virus type III in the acquired immune deficiency syndrome. Science **226**:1165–1171.

33. **Sodroski, J., R. Patarca, C. A. Rosen, F. Wong-Staal, and W. A. Haseltine.** 1985. Location of the *trans*-activating region of the genome of human T-cell lymphotropic virus type III. Science **229**:74–77.
34. **Sonigo, P., M. Alizon, K. Staskus, D. Klatzmann, S. Cole, O. Danos, E. Retzel, P. Tiollais, A. Haase, and S. Wain-Hobson.** 1985. Nucleotide sequence of the visna lentivirus: relationship to the AIDS virus. Cell **42**:369–382.
35. **Southern, P. J., and P. Berg.** 1982. Transformation of mammalian cells to antibiotic resistance with a bacterial gene under control of the SV40 early region promoter. J. Mol. Appl. Genet. **1**:327–341.
36. **Weiss, R.** 1982. Experimental biology and assay of RNA tumor viruses, p. 209–260. *In* R. Weiss, N. Teich, H. Varmus, and J. Coffin (ed.), RNA tumor viruses. Cold Spring Harbor Laboratory, Cold Spring Harbor, N.Y.
37. **Wigler, M., A. Pellicer, S. Silverstein, R. Axel, G. Urlaub, and L. Chasin.** 1979. DNA-mediated transfer of the adenine phosphoribosyltransferase locus into mammalian cells. Proc. Natl. Acad. Sci. USA **76**:1373–1376.
38. **Wong-Staal, F., G. M. Shaw, B. H. Hahn, S. Z. Salahuddin, M. Popovic, P. Markham, R. Redfield, and R. C. Gallo.** 1985. Genomic diversity of human T-lymphotropic virus type III (HTLV-III). Science **229**:759–762.
39. **Zavada, J., Z. Zavadova, G. Russ, K. Polakova, J. Rajcani, J. Stencl, and J. Loksa.** 1983. Human cell surface proteins selectively assembled into vesicular stomatitis virus virions. Virology **127**:345–360.

- Article
- Open Access
- Published: 16 April 2018

A single injection of crystallizable fragment domain–modified antibodies elicits durable protection from SHIV infection

Rajeev Gautam, Yoshiaki Nishimura, Natalie Gaughan, Anna Gazumyan, Till Schoofs, Alicia Buckler-White, Michael S. Seaman, Bruce J. Swihart, Dean A. Follmann, Michel C. Nussenzweig ✉ & Malcolm A. Martin ✉

Nature Medicine **24**, 610–616(2018)

Abstract

In the absence of an effective and safe vaccine against HIV-1, the administration of broadly neutralizing antibodies (bNAbs) represents a logical alternative approach to prevent virus transmission. Here, we introduced two mutations encoding amino acid substitutions (M428L and N434S, collectively referred to as 'LS') into the genes encoding the crystallizable fragment domains of the highly potent HIV-specific 3BNC117 and 10-1074 bNAbs to increase their half-lives and evaluated their efficacy in blocking infection following repeated low-dose mucosal challenges of rhesus

macaques (*Macaca mulatta*) with the tier 2 $SHIV_{AD8-EO}$. A single intravenous infusion of 10-1074-LS monoclonal antibodies markedly delayed virus acquisition for 18 to 37 weeks (median, 27 weeks), whereas the protective effect of the 3BNC117-LS bNAb was more modest (provided protection for 11–23 weeks; median, 17 weeks). Serum concentrations of the 10-1074-LS monoclonal antibody gradually declined and became undetectable in all recipients between weeks 26 and 41, whereas the 3BNC117-LS bNAb exhibited a shorter half-life. To model immunoprophylaxis against genetically diverse and/or neutralization-resistant HIV-1 strains, a combination of the 3BNC117-LS plus 10-1074-LS monoclonal antibodies was injected into macaques via the more clinically relevant subcutaneous route. Even though the administered mixture contained an amount of each bNAb that was nearly threefold less than the quantity of the single monoclonal antibody in the intravenous injections, the monoclonal antibody combination still protected macaques for a median of 20 weeks. The extended period of protection observed in macaques for the 3BNC117-LS plus 10-1074-LS combination could translate into an effective semiannual or annual immunoprophylaxis regimen for preventing HIV-1 infections in humans.

Main

Because an effective anti-HIV-1 vaccine is not currently available nor imminent, new approaches are needed to prevent HIV transmission. Such new strategies have included the use of bNAbs, isolated from infected persons with high titers of anti-HIV-1 neutralizing activity[1,2,3]. bNAbs are capable of neutralizing most circulating strains, targeting different nonoverlapping epitopes on the HIV-1 envelope spike, such as the CD4-binding site[3,4,5], variable loop 1 and 2 (V1V2 loop)[2,6], V3 loop[1,7,8], the membrane proximal region[9] and a series of epitopes spanning the gp120–gp41 interacting region[10,11]. Several bNAbs, including 3BNC117, VRC01, PGT121 and 10-1074, can protect macaques from simian–HIV (SHIV) infections[12,13,14,15,16,17]. In addition, these antibodies have been reported to control virus replication in chronically SHIV-infected

monkeys[18,19,20,21]. Human studies using the VRC01 or 3BNC117 monoclonal antibodies, which target the CD4-binding site, or the 10-1074 monoclonal antibody, which binds to the base of the gp120 V3 loop and surrounding glycans, have shown that the antibodies are generally safe and active in vivo[22,23,24,25]. bNAb administration transiently reduces plasma viremia and delays rebound during treatment interruption in individuals with an HIV-1 infection[22,23,24,25,26,27].

We previously reported that single intravenous (i.v.) injections of native VRC01, 3BNC117 or 10-1074 bNAbs (20 mg per kg body weight) prevented virus acquisition in macaques following repeated low-dose (RLD) challenges with tier 2 $SHIV_{AD8-EO}$ as compared to control monkeys that received no anti-HIV-1 neutralizing monoclonal antibodies[12]. In that study, the 3BNC117 and 10-1074 bNAbs protected monkeys for a median of 13 and 12.5 weeks, respectively, whereas VRC01, possessing lower neutralizing activity against $SHIV_{AD8-EO}$, blocked infection for a shorter period of time (a median of 8 weeks). In addition, the VRC01 monoclonal antibody, carrying a two-amino-acid substitution (LS) introduced into its crystallizable fragment domain that increased its serum half-life by two- to threefold[12,28], was also evaluated. As compared to the unmodified VRC01, the VRC01 monoclonal antibody with the LS substitution (VRC01-LS) exhibited a longer median protective effect (14.5 versus 8.0 weeks).

Here we have examined two aspects of anti-HIV-1 immunoprophylaxis: (1) the long-term efficacy of the more potent 3BNC117 or 10-1074 bNAbs with the LS substitution in the crystallizable fragment infused individually through the i.v. route; and (2) the prevention of virus acquisition via the combination of LS-mutant 3BNC117 and 10-1074 monoclonal antibodies administered subcutaneously (s.c.). Our results show that a single infusion of the 10-1074-LS monoclonal antibody protected four of six monkeys challenged on a weekly basis for more than 6 months. In addition and despite volume limitations (1.0 ml), s.c. combination immunoprophylaxis conferred protection in five of six monkeys against RLD virus challenge for a median of 20 weeks.

Results

Neutralizing potency of the LS-modified monoclonal antibodies

To examine the anti-$SHIV_{AD8\text{-}EO}$ neutralizing activity of the native[12] and LS-modified forms of 3BNC117 and 10-1074, we performed virus neutralization assays using either pseudotyped (Fig. 1a) or replication-competent (Fig. 1b) viruses during infections of TZM-bl cells. The half-maximal inhibitory concentrations (IC_{50}s) of the native and LS-modified forms of the 3BNC117 and 10-1074 monoclonal antibodies were nearly indistinguishable in the TZM-bl pseudovirus assay (0.07 versus 0.09 μg/ml and 0.08 versus 0.08 μg/ml, respectively). Similarly, assays using replication-competent $SHIV_{AD8\text{-}EO}$ showed IC_{50} values for the native and LS-modified forms of 3BNC117 and 10-1074 of 0.11 versus 0.11 μg/ml and 0.09 versus 0.08 μg/ml, respectively. The corresponding 80% inhibitory concentration (IC_{80}) values were 0.24 versus 0.37 μg/ml and 0.15 versus 0.15 μg/ml for native and LS-modified forms of 3BNC117 and 10-1074 monoclonal antibodies, respectively. We conclude that the LS-modified forms of 3BNC117 and 10-1074 have neutralization activities similar to those of the native antibodies in these in vitro assays.

Fig. 1: Neutralization sensitivity of broadly acting neutralizing anti-HIV-1 monoclonal antibodies against $SHIV_{AD8-EO}$.

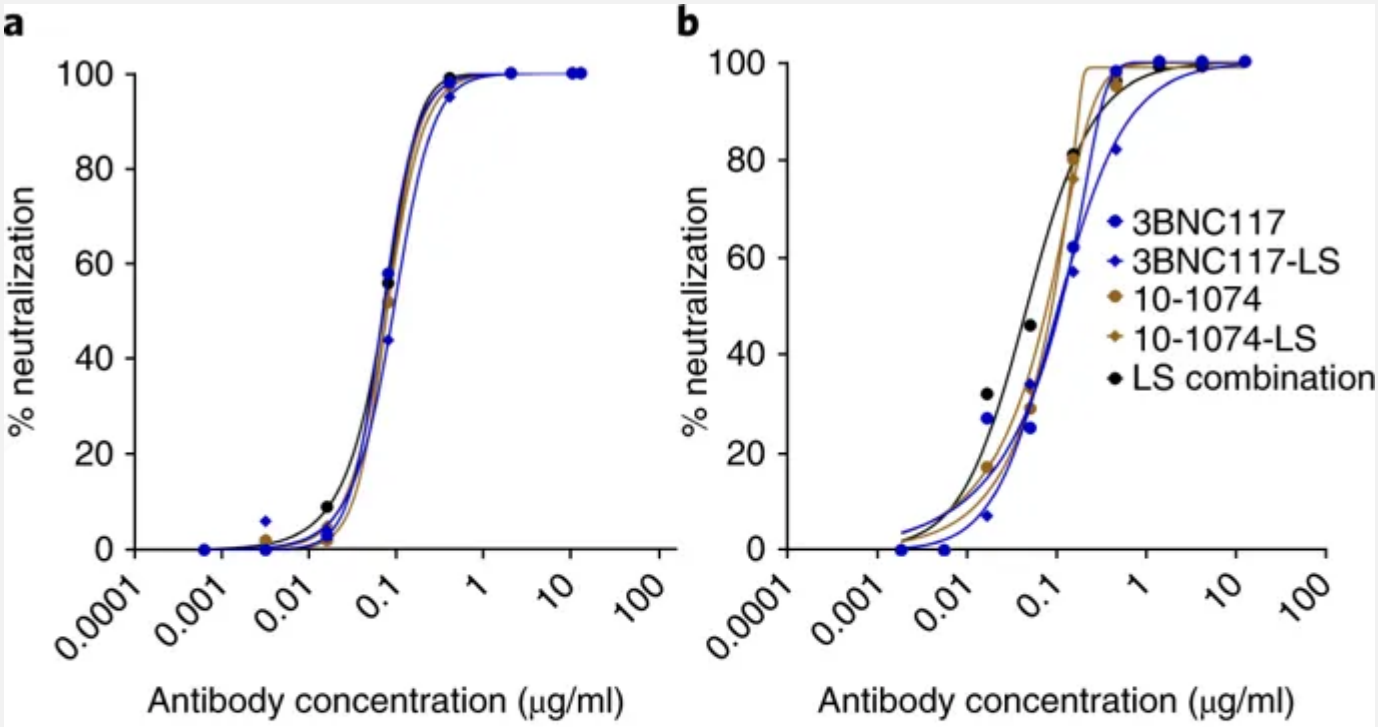

	IC_{50} (μg/ml)	IC_{80} (μg/ml)
3BNC117	0.07	0.13
3BNC117-LS	0.09	0.19
10-1074	0.08	0.14
10-1074-LS	0.08	0.15
LS combination	0.07	0.13

	IC_{50} (μg/ml)	IC_{80} (μg/ml)
3BNC117	0.11	0.24
3BNC117-LS	0.11	0.37
10-1074	0.09	0.15
10-1074-LS	0.08	0.15
LS combination	0.05	0.16

a, Top, neutralizing activity of the indicated bNAbs was determined against $SHIV_{AD8-EO}$ pseudovirions using TZM-bl target cells. Bottom, the calculated IC_{50} and IC_{80} values for the antibodies. **b**, Top, neutralizing activity of the indicated bNAbs was determined against replication-competent $SHIV_{AD8-EO}$ in a single-round TZM-bl infectivity assay in the presence of indinavir. Bottom, the calculated IC_{50} and IC_{80} values for the antibodies. The neutralization assays were repeated three times with similar results.

3BNC117-LS or 10-1074-LS monoclonal antibody administration confers long-term protection against repeated mucosal SHIV challenges

To determine the protective efficacy of 3BNC117-LS and 10-1074-LS monoclonal antibodies in macaques, we performed intrarectal (i.r.) RLD challenge experiments. All monkeys were inoculated with 10 tissue culture infectious dose 50 ($TCID_{50}$) of $SHIV_{AD8\text{-}EO}$ at weekly intervals until they became viremic, as determined through real-time RT-PCR analysis (Fig. 2a). This inoculum size was previously shown to be equivalent to 0.27 animal infectious dose 50 (AID_{50})[12]. Twelve control monkeys, which received no monoclonal antibodies, became infected after two to six challenges, with a median of three weekly virus exposures needed to infect all 12 monkeys (Fig. 2b). The protective efficacy of 3BNC117-LS or 10-1074-LS was assessed following a single i.v. infusion of each monoclonal antibody (20 mg per kg body weight) in six monkeys. The macaques were challenged beginning one week after bNAb administration, and in addition to levels of viral RNA, we measured serum bNAb concentrations, anti-SHIV neutralizing titers and anti-bNAb responses.

Fig. 2: Crystallizable fragment domain–modified HIV monoclonal antibodies confer durable protection against repeated low-dose IR $SHIV_{AD8-EO}$ challenges.

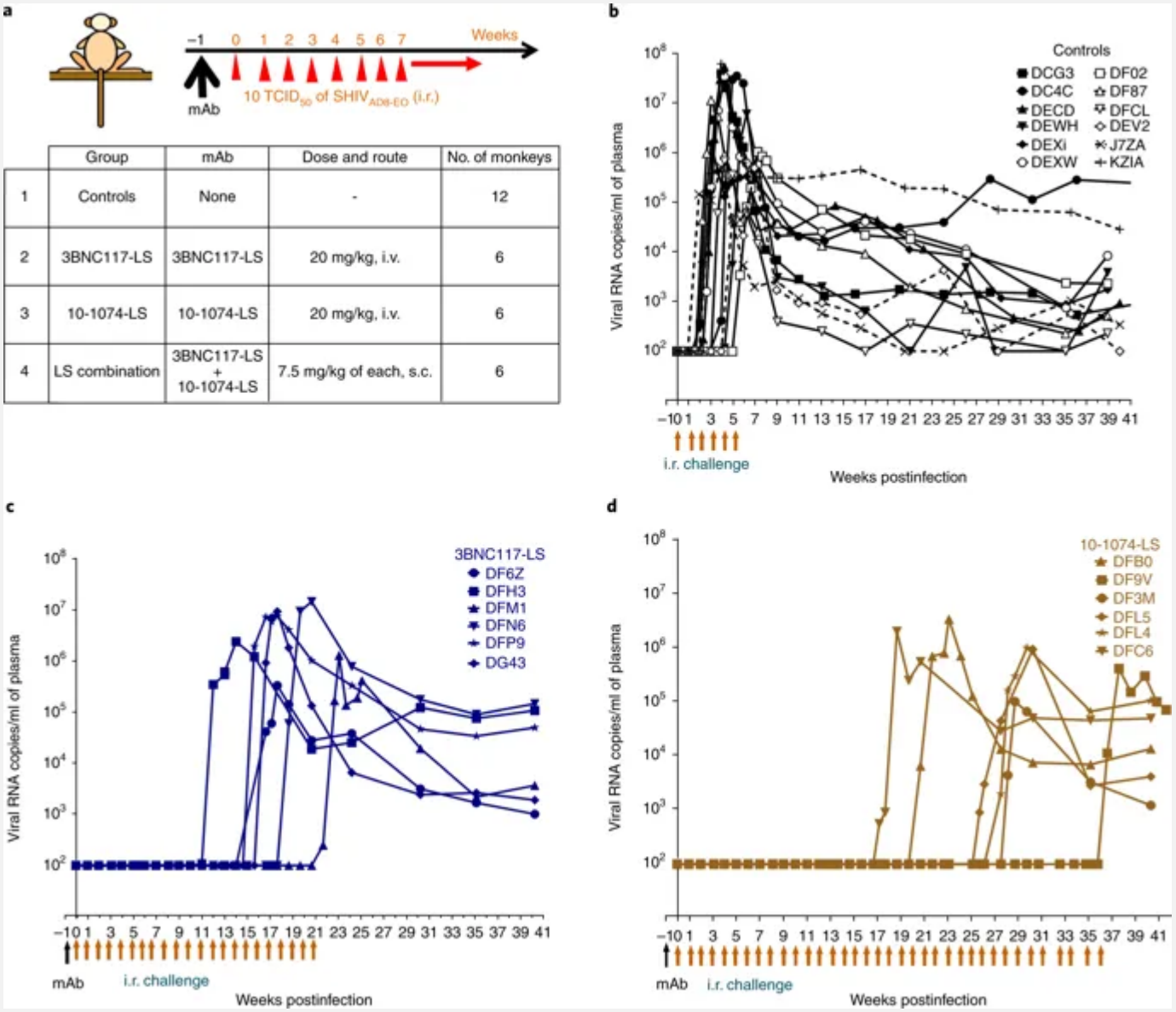

	Group	mAb	Dose and route	No. of monkeys
1	Controls	None	-	12
2	3BNC117-LS	3BNC117-LS	20 mg/kg, i.v.	6
3	10-1074-LS	10-1074-LS	20 mg/kg, i.v.	6
4	LS combination	3BNC117-LS + 10-1074-LS	7.5 mg/kg of each, s.c.	6

a, Experimental design for assessment of the protective efficacy of monoclonal antibodies in rhesus macaques. Single doses of the indicated individual monoclonal antibodies (20 mg per kg body weight) or combination monoclonal antibodies (7.5 mg per kg body weight of each monoclonal antibody) were administered either i.v. or s.c. Macaques were challenged with $SHIV_{AD8-EO}$ via the i.r. route weekly, beginning 1 week following monoclonal antibody (mAb) infusion. **b**, Plasma viral loads in rhesus macaques receiving no monoclonal antibody (controls; *n* = 12) challenged weekly with $SHIV_{AD8-EO}$. **c**,**d**, Plasma viral loads in rhesus macaques (*n* = 6 per group) challenged

weekly with $SHIV_{AD8-EO}$ beginning 1 week after i.v. administration of 3BNC117-LS (**c**) or 10-1074-LS (**d**) monoclonal antibody.

The LS-modified bNAbs were well tolerated in all 12 monkeys. In the six 3BNC117-LS bNAb recipients, 11 to 23 challenges were required to establish infection, and the median time to virus acquisition was 17 weeks for this group of monkeys (Fig. 2c). In the case of the 10-1074-LS recipients, 18 to 37 virus challenges were needed to establish an infection, and the median time to virus acquisition was 27 weeks (Fig. 2d). The median times to virus acquisition in the recipients of the native 10-1074 and 3BNC117 monoclonal antibodies were 12.5 and 13 weeks, respectively[12]. Thus, the 10-1074-LS bNAb conferred a 2.2-fold increase (12.5 to 27) in the number of challenges needed to establish an infection compared with the unmodified 10-1074 monoclonal antibody, whereas the 3BNC117-LS bNAb conferred a modest 1.3-fold (13 to 17 challenges) improvement. The protective effects of the 3BNC117-LS and 10-1074-LS bNAbs were also compared to the control cohort using Kaplan–Meier analysis, in which the percentage of macaques remaining uninfected was plotted against the number of $SHIV_{AD8-EO}$ challenges (Fig. 3a). As indicated in Fig. 3b, the recipients of 3BNC117-LS and 10-1074-LS monoclonal antibodies were significantly more resistant to $SHIV_{AD8-EO}$ acquisition than the control monkeys ($P = 0.004$ and 0.004, respectively). Furthermore, 10-1074-LS was significantly different from native 10-1074 ($P = 0.026$), whereas the 3BNC117-LS was not statistically different from its native form ($P = 0.108$).

Fig. 3: Protective effects of 3BNC117-LS and 10-1074-LS monoclonal antibodies against virus acquisition in rhesus macaques.

a

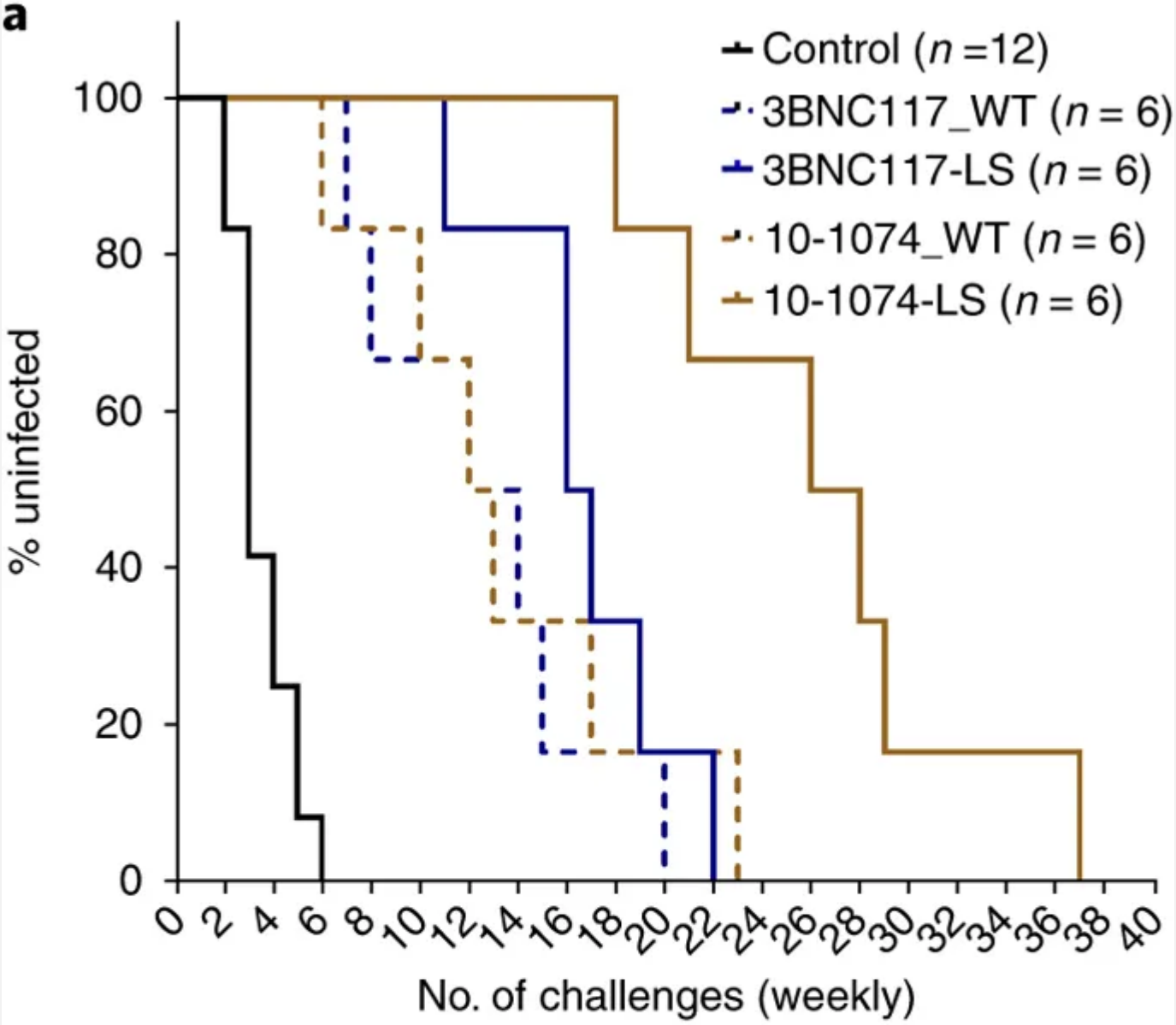

b

Groups compared		Wilcoxon *P* value
Control	3BNC117-LS	0.004
Control	10-1074-LS	0.004
3BNC117	3BNC117-LS	0.108
10-1074	10-1074-LS	0.025
3BNC117-LS	10-1074-LS	0.040

a, Kaplan–Meier analysis was used to assess infection rates for controls and recipients of 3BNC117-LS and 10-1074-LS monoclonal antibodies and their native forms. The

percentage of uninfected rhesus macaques following $SHIV_{AD8-EO}$ i.r. challenge was assessed for the monoclonal antibody recipients (n = 6 per group) and control monkeys (n = 12). **b**, P values were determined using Wilcoxon rank-sum test (two-sided) comparing the number of challenges resulting in infections of control monkeys versus the individual monoclonal antibody–recipient group or between different monoclonal antibody–recipient groups.

In vivo protective activity is dependent upon monoclonal antibody pharmacokinetics

To determine how LS-modified bNAbs in monkey sera relate to protection, we measured the concentrations of these antibodies at various times after administration. The serum concentrations of 3BNC117-LS in five of six recipients gradually declined and became undetectable between weeks 16 and 22 following infusion (Fig. 4a and Supplementary Table 1). One 3BNC117-LS monoclonal antibody recipient (DFH3), however, experienced rapid decay of the administered antibody, and the monoclonal antibody concentrations in this monkey declined to undetectable levels by week 5 postinfusion. In contrast, none of the six macaques infused with the 10-1074-LS bNAb exhibited a rapid loss of the administered monoclonal antibodies; bNAbs were measurable until weeks 26–41 in this cohort of monkeys (Fig. 4b and Supplementary Table 1). The median serum-neutralizing activities of the 3BNC117-LS and 10-1074-LS monoclonal antibodies 1 week after infusion were 1:2,538 and 1:9,840, respectively (P = 0.0022, Wilcoxon rank-sum test; Supplementary Fig. 1). These values are similar to comparable titers (1:3,248 and 1:7,163) measured at 1 week following infusion of the native 3BNC117 and 10-1074 bNAbs, respectively[12]. Thus, despite exhibiting similar neutralization activities against $SHIV_{AD8-EO}$ in vitro (Fig. 1), the neutralization titers of each bNAb at 1 week following infusion were different from one another in vivo, with higher titers measured for native 10-1074 and 10-1074-LS compared to native 3BNC117 and 3BNC117-LS.

Fig. 4: Serum antibody concentrations in rhesus macaques infused with crystallizable fragment domain–modified monoclonal antibodies.

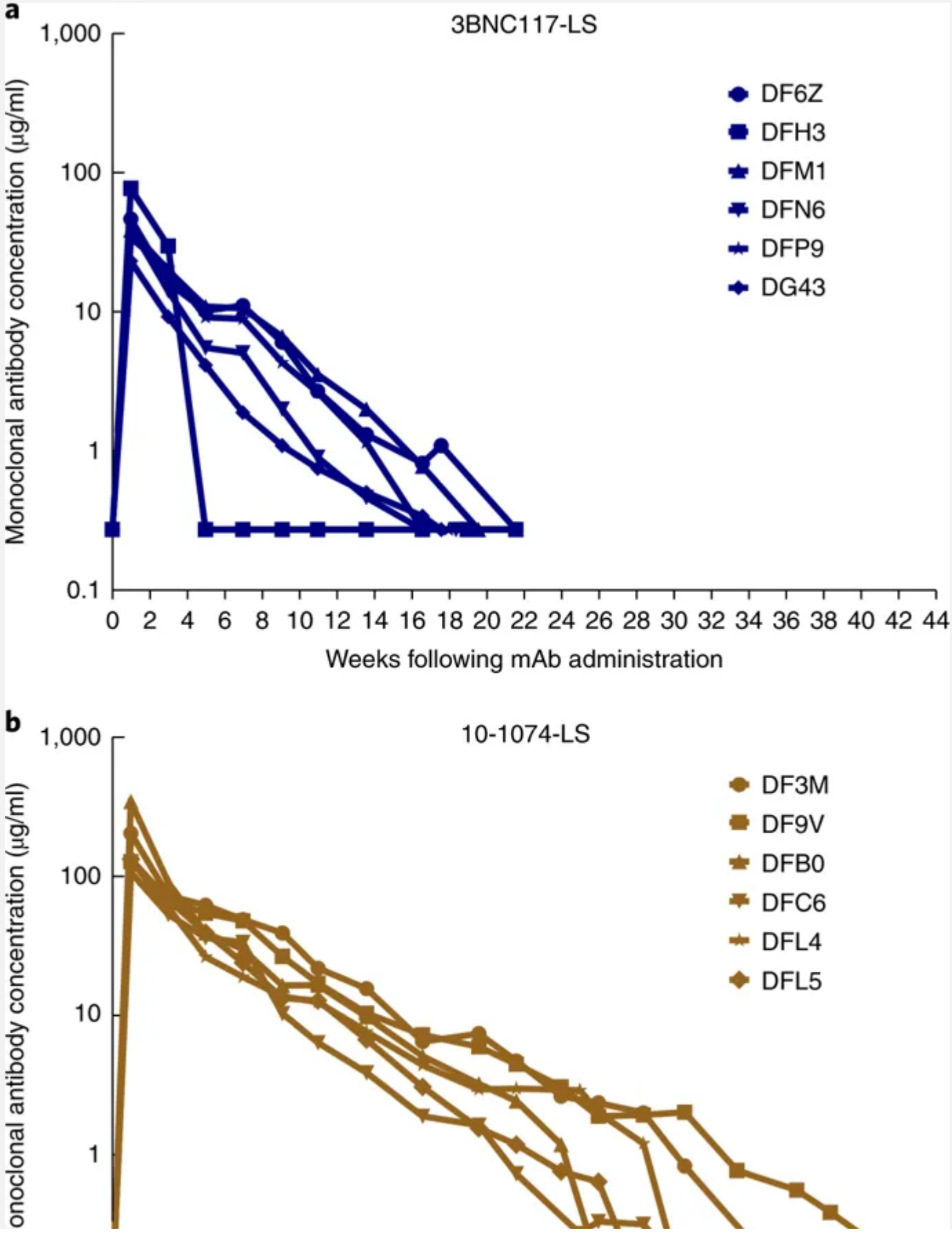

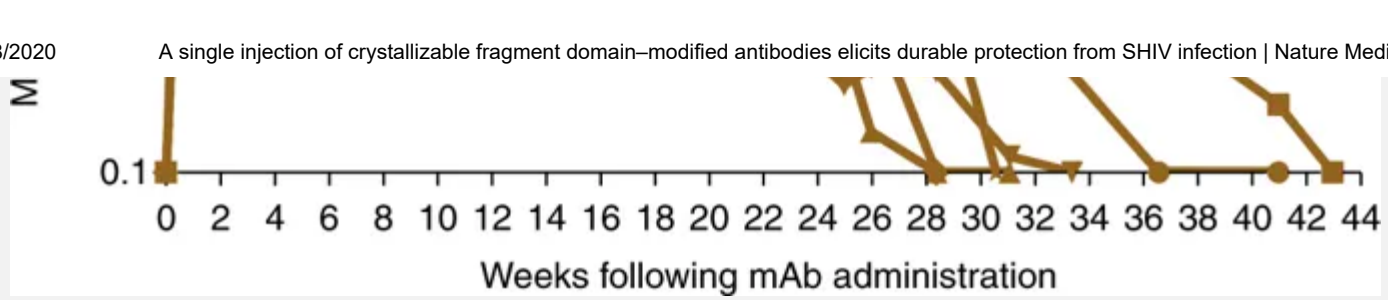

a, Concentrations of 3BNC117-LS antibody were measured in serum over the course of 6 months following a single i.v. infusion (20 mg per kg body weight) of the 3BNC117-LS monoclonal antibody using the TZM-bl cell assay. **b**, Concentrations of 10-1074-LS antibody were measured in serum for 9 months after i.v. infusion of a single 20 mg per kg body weight dose of 10-1074-LS monoclonal antibody using a TZM-bl cell assay. The assay was performed twice.

The introduction of the LS-encoding mutations into the gene encoding VRC01 extended its serum half-life by two- to threefold[12,28]. The half-life of 3BNC117-LS ranged from 1.5 to 3.2 weeks (median, 2.8 weeks), whereas native 3BNC117 had a half-life of 0.7 to 1.7 weeks (median, 1.4 weeks), as shown in Supplementary Table 2. Similarly, the half-life of 10-1074-LS ranged from 3.0 to 4.9 weeks (median, 3.8 weeks) and the native monoclonal antibody exhibited a half-life of 0.6 to 3.2 weeks (median, 1.0 week), as shown in Supplementary Table 2. Thus, the LS-encoding mutation increased the half-lives of native 3BNC117 and 10-1074 by 2.0- and 3.8-fold, respectively ($P = 0.0044$ for 3BNC117-LS versus 3BNC117 and $P = 0.0014$ for 10-1074-LS versus 10-1074).

bNAb combination immunoprophylaxis prevents SHIV acquisition

In view of the extraordinary genetic diversity of HIV-1, it is likely that prophylaxis against HIV-1 in humans will require a combination of bNAbs targeting different epitopes on the viral envelope. In addition, i.v. antibody administration is far less desirable as a means of prophylaxis in humans than injection via the s.c. route. To evaluate the protective efficacy of combining bNAbs, we administered 3BNC117-LS plus 10-1074-LS monoclonal antibodies (7.5 mg per kg body weight of each) in a clinically

relevant volume of 1 ml s.c. to a cohort of six macaques, which were challenged weekly with 10 $TCID_{50}$ of $SHIV_{AD8\text{-}EO}$, as described above. This monoclonal antibody dose was nearly three times lower than that used when each bNAb was i.v. administered individually (20 mg per kg body weight of each), as described earlier. As shown in Fig. 5a, combination monoclonal antibody prophylaxis conferred protection for 15 to 24 challenges in five of the six recipients. One monkey (DFM6) became infected after only six i.r. challenges. The median time to virus acquisition for the entire cohort was 20 weeks ($P = 0.004$ compared to untreated controls, Wilcoxon rank-sum test; Fig. 5b).

Fig. 5: Protection efficacy of combination 3BNC117-LS plus 10-1074-LS monoclonal antibody administered s.c. to rhesus macaques.

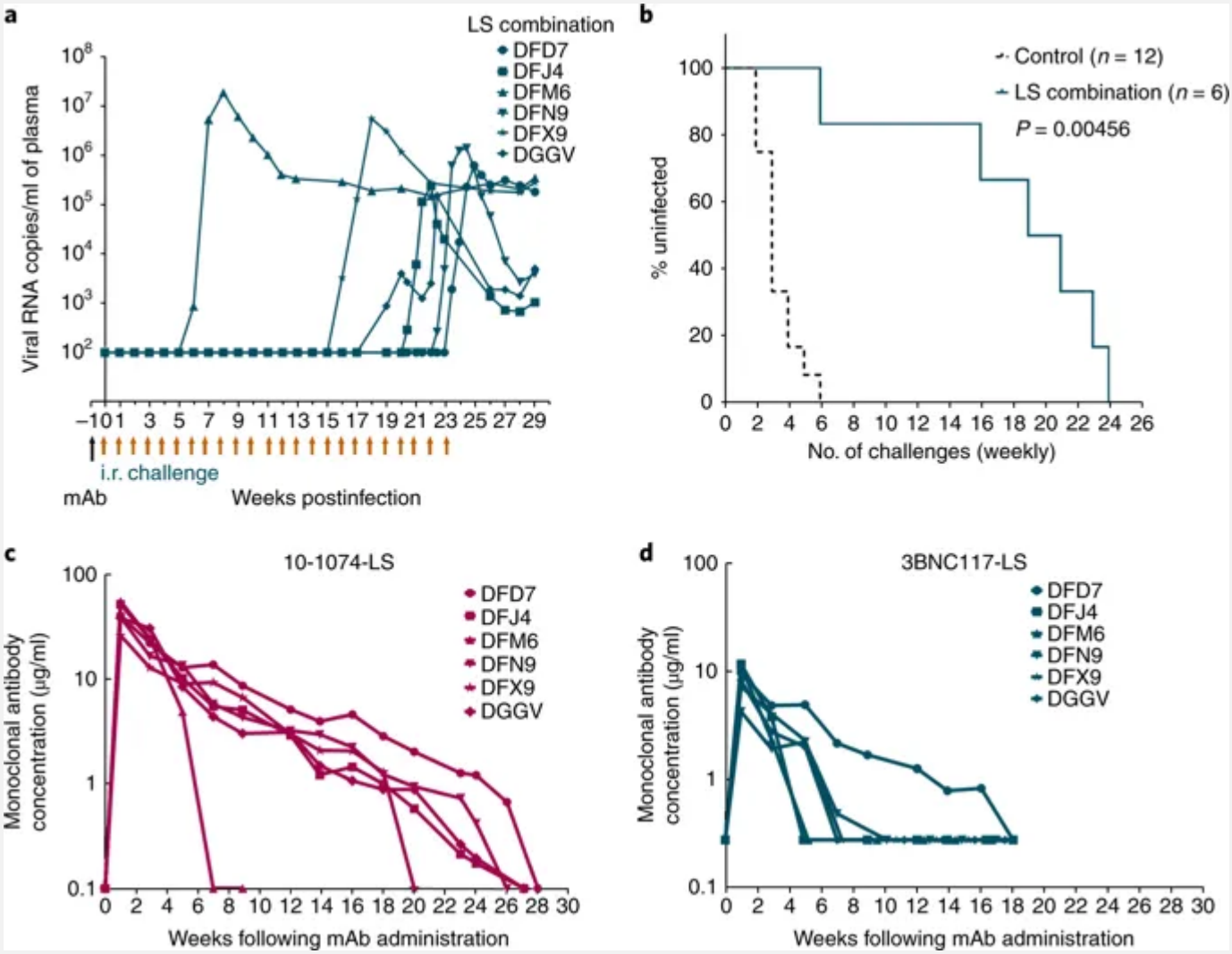

a, Plasma viral loads in rhesus macaques (n = 6) challenged repeatedly with $SHIV_{AD8\text{-}EO}$ beginning 1 week after the s.c. administration of a single dose of the 3BNC117-LS plus 10-1074-LS monoclonal antibody mixture (7.5 mg per kg body weight of each). **b**, Kaplan–Meier survival curves show the percentage of rhesus macaques remaining uninfected following repeated $SHIV_{AD8\text{-}EO}$ i.r. challenges required to establish infection of monoclonal antibody–combination recipients (n = 6) or controls (n = 12). P values were determined using the Wilcoxon rank-sum test (two-sided) comparing the number of challenges resulting in infection of the controls and monoclonal antibody–combination recipients. **c**,**d**, Concentrations of 10-1074-LS and 3BNC117-LS monoclonal antibodies were measured, using the TZM-bl cell assay, in serum of rhesus macaques

administered a single injection of the monoclonal antibody mixture s.c. Antibody concentrations were measured twice.

The concentrations of the 3BNC117-LS and 10-1074-LS monoclonal antibodies in sera from individual macaques were determined longitudinally (Fig. 5c,d). The serum concentrations of 3BNC117-LS monoclonal antibody declined to undetectable levels between 5 and 9 weeks in all but one of the six recipients (Fig. 5d and Supplementary Table 3). The sixth monkey, DFD7, maintained measurable concentrations of the 3BNC117-LS monoclonal antibody until week 18 following s.c. administration. In contrast, the 10-1074-LS bNAb gradually declined in five of the six monkeys and was detected in circulation until weeks 18–27 post administration in all five of these monkeys (Fig. 5c and Supplementary Table 3). One macaque (DFM6) experienced rapid loss of both monoclonal antibodies and became infected after six weekly challenges (Fig. 5a). The pattern of anti-HIV-1 serum neutralizing titers in recipients of the 3BNC117-LS plus 10-1074-LS monoclonal antibody mixture paralleled the serum concentrations of the 10-1074-LS monoclonal antibody, but not that of the 3BNC117-LS monoclonal antibody, in this macaque cohort (compare Supplementary Fig. 2 with Fig. 5c,d). Taken together, these results show that the 10-1074-LS monoclonal antibody was solely responsible for the protection of five of the six macaques after week 7.

Monoclonal antibody concentration and neutralization activity predict the probability of infection

We used probit regression analysis to estimate an S-shaped curve that describes the per-challenge probability of infection as a function of the serum monoclonal antibody concentration (Supplementary Tables 1 and 3). The estimated probit curve for these studies is shown in Fig. 6a. Likelihood ratio tests indicated that the same probit curve could be applied for each of the following monoclonal antibodies: native 3BNC117 and 3BNC117-LS; native 10-1074 and 10-1074-LS; and the 3BNC117-LS plus 10-1074-LS combination. Thus, a given amount of monoclonal antibody from any of the five types

evaluated predicted the same per-challenge infection probability. The serum monoclonal antibody concentration, corresponding to a per-challenge infection probability of 1%, was calculated to be 2.67 μg/ml (95% confidence interval, 1.85–3.48 for all of the monoclonal antibodies evaluated). As shown in Fig. 6b, the median monoclonal antibody serum concentrations at breakthrough of infection were calculated to be 0.13 and 1.07 μg/ml for native 10-1074 and 10-1074-LS, respectively; 0.20 and 0.28 μg/ml for native 3BNC117 and 3BNC117-LS, respectively; and 0.67 μg/ml for the bNAb combination. The slightly higher breakthrough plasma bNAb concentration observed for the 10-1074-LS monoclonal antibody (1.07 μg/ml) compared to the three other individual bNAbs analyzed in Fig. 6b cannot be presently explained despite the similar potencies of these antibodies when measured in vitro (Fig. 1). Perhaps this difference reflects currently unknown variables affecting bNAb activity in vivo that are not operative in vitro.

Fig. 6: Antibody concentration predicts the probability of infection.

a, Probit regression was used to model the probability of infection based on antibody concentrations in serum of rhesus macaques at the time of each $SHIV_{AD8\text{-}EO}$ challenge. The probability of infection for the control monkeys (*n* = 12) was estimated to be 0.27. The fitted probability, determined using the probit regression model, is plotted for all recipients of LS-modified monoclonal antibodies (*n* = 18) and native monoclonal antibodies (*n* = 12; previously reported[12]). Each red circle indicates the monoclonal antibody concentration at the time of virus challenge resulting in infection; blue circles indicate the monoclonal antibody concentration at the time of virus challenge not resulting in infection. A monoclonal antibody concentration of 2.67 μg/ml in serum was predicted to have a 0.01 per-challenge infection probability. **b**, Concentrations of monoclonal antibodies in sera from rhesus macaques at the time of virus acquisition. The tops and bottoms of each box represent 75th and 25th percentiles, respectively. The bars above and/or below each box (whiskers) represent the entire spread of the data points, and the heavier line represents the median value for each group (*n* = 6 per group, except for controls, where *n* = 12). Some of the data points on the box plots are superimposed.

The protective efficacy of different serum antibody concentrations, relative to the per-challenge risk of infection, was also determined. Antibody efficacy was defined as 100% × ((1 − (per-challenge infection probability at a given antibody concentration)) / (per-challenge infection probability with no antibody)) (see statistical analysis in the Methods for details). The antibody efficacies were 97% (95% confidence interval, 92–100%) and 61% (95% confidence interval, 49–77%) for all of the wild-type and crystallizable fragment domain–modified 3BNC117 and 10-1074 bNAbs used in this study at serum concentrations of 3.0 and 1.0 μg/ml, respectively.

Anti-antibody responses against human monoclonal antibodies can cause their rapid decay in macaques

Macaque recipients of human anti-HIV-1 bNAbs variably produce anti-antibodies that are associated with accelerated bNAb clearance, and in prevention experiments, this leads to virus acquisition[12]. In the current study, one monkey (DFH3), in the cohort of six 3BNC117-LS monoclonal antibody recipients, developed anti-antibodies at 3 to 4 weeks after infusion and experienced a decline of bNAb concentrations to undetectable levels by week 5 (Fig. 4a and Supplementary Fig. 3a). The most striking example of anti-antibody production occurred in the bNAb combination experiment, where four of six monkeys developed specific anti-3BNC117-LS antibodies after 4 to 6 weeks, and one of these macaques (DFM6) also produced anti-antibodies to the 10-1074-LS component of the mixture in a similar time frame (Supplementary Fig. 3c,d). As expected, the generation of anti-antibodies against both 3BNC117-LS and 10-1074-LS monoclonal antibodies in monkey DFM6 was associated with a rapid decline of both serum bNAb concentrations (Fig. 5c,d) and measurable neutralization titers in this animal (Supplementary Fig. 2), resulting in the establishment of infection.

Discussion

The most striking result obtained in this study is the long period of protective efficacy conferred by a single injection of crystallizable fragment domain–modified human anti-HIV-1 neutralizing antibodies in macaques compared to that previously reported[12]. A single i.v. infusion of the 10-1074-LS bNAb protected a cohort of six monkeys for up to 8.5 months (18–37 weeks). The introduction of the LS substitution into 10-1074 lengthened the median time until $SHIV_{AD8\text{-}EO}$ acquisition from 12.5 to 27 weeks. The administered 10-1074-LS bNAb was measurable in the serum for 26–41 weeks and had a calculated half-life of 3.8 weeks.

The effects of LS on 3BNC117 were more modest than those on 10-1074 and were consistent with a shorter half-life (2.6 versus 3.8 weeks), a smaller increase in half-life

(2- versus 3.8-fold) and a lower initial serum concentration (Supplementary Table 2). These observations are also entirely in accordance with the observation that native 3BNC117 has a shorter half-life than 10-1074 in humans (17 versus 24 d)[22,23]. This difference in pharmacokinetics notwithstanding, a serum concentration of 2.68 μg/ml for either LS-modified bNAb derivative was calculated to protect 99% of the macaque recipients.

We tested combination immunoprophylaxis via the s.c. route, employing the 3BNC117-LS plus 10-1074-LS monoclonal antibodies, which target different gp120 epitopes, to model potential exposure to genetically diverse and/or resistant HIV-1 strains. Unexpectedly, four of six of these monkeys developed high titers of anti-3BNC117-LS antibodies within 5–9 weeks of administration, which resulted in the rapid elimination of this monoclonal antibody. This loss of the 3BNC117-LS component of the bNAb combination could be viewed as the biological equivalent of the previously reported emergence of viral variants resistant to an administered anti-HIV-1 monoclonal antibody[20,23,26,27,29,30]. Nonetheless, the inclusion of 10-1074-LS in the administered bNAb combination resulted in the maintenance of neutralizing activity in serum for several months, prevented the establishment of a virus infection for an additional 6–14 weeks and was solely responsible for the observed protection (median, 20 weeks) in this cohort of $SHIV_{AD8\text{-}EO}$-challenged macaques.

Development of anti-antibodies against the administered human bNAbs in macaques was not unexpected. In fact, bNAb concentrations and neutralization titers invariably declined in 15 of the 24 monkeys infused with 3BNC117-LS and/or 10-1074-LS monoclonal antibodies when anti-bNAb titers exceeded a titer of 1:1,000 (Supplementary Fig. 3a–d). Although the generation of such antibodies will always remain a problem in the context of monkey recipients of human monoclonal antibodies, it is highly unlikely that a cross-species immune response of this frequency and potency and the attending rapid clearance of administered bNAbs will occur in humans. In this regard, two recent clinical studies have reported that VRC01 administered to healthy human adults failed to elicit detectable anti-antibodies[24,25],

and 3BNC117 and 10-1074 showed stable pharmacokinetics in humans after repeated dosing over a period of 6 months (data not shown).

Before the development of an effective vaccine against hepatitis A virus, pre-exposure immunoprophylaxis through administering immunoglobulin intramuscularly was common practice and conferred protection for 3–5 months[31]. In the absence of an effective HIV vaccine or the development of one in the immediate future, it is not unreasonable to contemplate a similar use of crystallizable fragment domain–modified anti-HIV monoclonal antibodies, such as those described in this report, which, in the case of 10-1074-LS bNAb, conferred protection in macaques against $SHIV_{AD8-EO}$ for more than 6 months.

Although this study reports a promising preclinical result relevant to HIV-1 prevention, it must be remembered that to be clinically effective for immunoprophylaxis, bNAbs must be capable of preventing the acquisition of genetically diverse populations of the virus, not a molecularly cloned SHIV expressing a single envelope protein. The planned extension of the LS-modified bNAb results reported here to humans in a phase 1 clinical trial to evaluate the pharmacokinetics of 3BNC117-LS administered to groups of individuals with and without HIV infections thus represents the next step in this process (http://www.clinicaltrials.gov/; NCT03254277).

Methods

Rhesus monkeys

Thirty rhesus macaques (*Macaca mulatta*) of Indian genetic origin, 2–4 years of age, were housed and cared for in accordance with Guide for Care and Use of Laboratory Animals Report no. NIH 82-53 (Department of Health and Human Services, Bethesda, Maryland, 1985) in a biosafety level 2 NIH facility. All animal procedures and experiments were performed according to protocols approved by the Institutional

Animal Care and Use Committee of National Institute of Allergy and Infectious Disease, NIH. Monkeys were not randomized, and the data were not collected in a blinded manner. The macaques used in this study did not express the MHC class I Mamu-A*01, Mamu-B*08 and Mamu-B*17 alleles. No monkeys were excluded from the analysis. Nine of the twelve control monkeys and recipients of the native 3BNC117 (n = 6) and 10-1074 (n = 6) bNAbs were reported in a previous study[12]. Blood was drawn regularly to monitor viral infection, passively transferred monoclonal antibody concentrations and serum neutralizing activity.

Monoclonal antibodies

The 3BNC117 monoclonal antibody is a recombinant, fully human IgG1 λ antibody recognizing the CD4-binding site on the HIV-1 gp120 envelope[5]. This antibody was cloned from an HIV-1-infected viremic controller in the International HIV Controller Study[5,32], and the mutations encoding the LS substitution were introduced to the heavy chain–encoding gene of 3BNC117 bNAb through site-directed mutagenesis. Plasmids encoding the heavy and light chain genes were transiently cotransfected and expressed in Chinese hamster ovary cells (clone 5D5-5C10), and supernatant was purified using standard methods. The resulting purified monoclonal antibody, designated 3BNC117-LS, was used for i.v. and s.c. injections of macaques. 10-1074 is a recombinant, fully human IgG1 λ monoclonal antibody recognizing the base of the gp120 V3 loop and surrounding glycans on the HIV-1 envelope protein[8]. The 10-1074 monoclonal antibody was cloned from an African donor (patient 10) infected with an HIV-1 clade A virus[33]. LS-encoding mutations were introduced into the heavy chain–encoding gene of 10-1074, expressed in Chinese hamster ovary cells (clone 3G4), and the purified bNAb, designated 10-1074-LS, was used in the study. A single dose (20 mg per kg body weight) of each monoclonal antibody was infused i.v. to individual monkeys.

To model immunoprophylaxis via the more clinically relevant s.c. route, a bNAb combination, which included both 3BNC117-LS and 10-1074-LS monoclonal antibodies

(7.5 mg per kg body weight of each), in a total volume of 1 ml, was administered s.c. into the medial inner thigh of individual animals using a 1-inch, 25-gauge needle.

Virus challenge

The origin and preparation of the tissue-culture-derived $SHIV_{AD8-EO}$ stock has been previously described[34]; the infectivity of virus stock was titrated on peripheral blood mononuclear cells (PBMCs) from rhesus macaques. $SHIV_{AD8-EO}$ is an molecularly cloned derivative of $SHIV_{AD8}$ that is R5 tropic and possesses multiple properties typical of pathogenic HIV-1 isolates[34,35,36]. It exhibits a tier 2 neutralization-sensitivity phenotype, replicates to high levels in rhesus macaque PBMCs, generates sustained levels of plasma viremia and causes irreversible depletion of $CD4^+$ T cells, resulting in a symptomatic and ultimately fatal immunodeficiency associated with opportunistic infections (*Mycobacterium* sp., *Pneumocystis* sp., *Cryptosporidium* sp.) in infected monkeys. All animals were inoculated through the i.r. route with 10 $TCID_{50}$ of $SHIV_{AD8-EO}$ at weekly intervals until infection became established. This inoculum size was previously shown to be equivalent to 0.27 AID_{50}[12]. A pediatric speculum was used to gently open the rectum, and a 1-ml suspension of virus in a tuberculin syringe was slowly infused into the rectal cavity.

Neutralization antibody assay

The in vitro potency of each monoclonal antibody was assessed using two types of neutralization assays: (1) TZM-bl entry assay with a pseudotyped virus and (2) TZM-bl infection assay using a replication-competent virus. The pseudotyped virus expresses the $SHIV_{AD8-EO}$ envelope antigen and the luciferase reporter gene. In the case of the replication-competent virus assay, the indinavir protease inhibitor was added to the medium (final concentration of 1 μM) to prevent a second round of viral replication. Neutralization activity was quantitated by the relative decrease in the luciferase activity compared to infection of TZM.bl cells in the absence of monoclonal antibodies. Neutralization curves were subjected to fitting through nonlinear regression using a

five-parameter equation using GraphPad Prism. The antibody concentrations required to inhibit infection by 50% or 80% are reported as the IC_{50} or IC_{80}, respectively.

Measurement of 3BNC117-LS and 10-1074-LS monoclonal antibody concentrations

Serum concentrations of 3BNC117-LS and 10-1074-LS bNAbs were determined using TZM.bl neutralization assays as previously described[23]. Sera were heat-inactivated for 1 h at 56 °C, and neutralizing activity was measured against two HIV-1 strains. HIV-1 strain Q769.d22 is highly sensitive to 3BNC117 but resistant to 10-1074, whereas the X2088_c9 strain is highly sensitive to 10-1074 but resistant 3BNC117. ID_{50} values were derived using five-parameter curve fitting. Serum concentrations of 3BNC117-LS and 10-1074-LS were then calculated through multiplying the respective sera ID_{50} titers by the IC_{50} values. Murine leukemia virus (MuLV)-pseudotyped viruses were used to detect nonspecific neutralizing activity in serum, which was excluded from analyses.

Measurement of 3BNC117-LS and 10-1074-LS neutralizing activity

The neutralization activity, present in serum samples collected from rhesus macaques infused with monoclonal antibodies, was assessed through TZM-bl assay with pseudotyped $SHIV_{AD8}$[12,16]. The IC_{50} neutralization titer was calculated as the dilution of serum causing a 50% reduction in relative luminescence units (RLUs) relative to diluted sera from untreated animals.

Pharmacokinetic analysis

Blood samples were collected before and weekly following administration of the bNAbs. Monoclonal antibody serum concentrations were determined as described above. Pharmacokinetic parameters were estimated by performing a non-compartmental analysis using WinNonlin 6.3.

Anti-antibody responses

ELISAs were performed to evaluate anti-3BNC117-LS or anti-10-1074-LS antibody responses in sera collected from macaques administered these monoclonal antibodies. ELISA plates (96 well) were coated with 3BNC117-LS or 10-1074-LS monoclonal antibodies in PBS (2 μg/ml), incubated at 4 °C overnight and blocked with 5% BSA at room temperature for 1 h. Plates were washed six times with PBS-Tween (PBS-T), and serial, fivefold dilutions of serum samples were prepared in 2% BSA. The diluted serum samples were added to plates and incubated at room temperature for 1 h, followed by six washes of each plate with PBS-Tween. Horseradish peroxidase (HRP)-conjugated Fcγ-specific anti–human IgG, (Jackson ImmunoResearch Labs) was added for 1 h at room temperature, followed by six washes of each plate with PBS-T. Tetramethylbenzidine (TMB)–HRP substrate was added to each well, and the absorbance developed after adding 0.5 M H_2SO_4 was measured at 450 nm on a EMax Plus Microplate Reader using Softmax Pro 6 software (Molecular Devices, CA, US). Blank wells containing assay diluent were used to determine the background signal; mean optical density (OD) values exceeding fivefold (ranging from 0.26 to 0.29) that of blank wells from each plate were used as cutoff. The dilution of each sample above the cutoff value was then calculated. The log values of these dilutions were reported as the final endpoint anti-bNAb titers.

Plasma viral RNA quantification

Plasma viral RNA levels were determined through modified two-step quantitative reverse transcription using Applied Biosystems PCR (ABI Prism 7900HT). Experimental samples were analyzed in parallel with a simian immunodeficiency virus (SIV) gag RNA standard; the lower limit of detection using this assay was 100 copies/ml.

Cell culture

HEK293T and TZM.bl cells were maintained in the DMEM media supplemented with 10% FBS, 4 mM L-glutamine and 1 × penicillin–streptomycin. Cells were passaged twice a week and incubated at 37 °C, 10% CO_2.

Statistical analysis

Between-group comparisons were performed using the Wilcoxon rank-sum test. The relationship between per-challenge infection and antibody concentration at the time of challenge was specified by a probit regression model: P(infection at challenge) = Φ(A + B mAb), where A and B are parameters to be estimated; mAb is the actual or imputed antibody concentration at the time of the challenge; and Φ is the standard normal cumulative distribution function. Because the monoclonal antibody concentrations were missing for some challenges, a linear mixed-effects model was fitted to the repeated monoclonal antibody readouts. Empirical Bayes–predicted monoclonal antibody concentrations were used to impute values for challenges with missing monoclonal antibody readouts. ID01 was defined as the antibody concentration resulting in an estimated per-challenge probability of infection of 0.01.

Likelihood ratio tests were performed to examine whether the different groups of monoclonal antibodies (native-10-1074, 10-1074-LS, native-3BNC117, 3BNC117-LS and combination of the two LS-modified bNAbs) had different slopes and intercepts. For each group, in turn, separate models were fitted to allow for a group-specific intercept and a group-specific intercept and slope. For each group, likelihood-ratio tests supported the simpler model with a single intercept and slope for all groups ($P > .05$). Additional likelihood-ratio tests were performed to confirm that other functions (i.e., log, quadratic) of the infused monoclonal antibody did not provide a significantly better prediction. A random-effects probit model was also assessed, and the variance of the intercept term was estimated at zero.

We calculated the reduction in the per-challenge probability of infection for a given antibody concentration, as compared to that with no antibody, using the formula antibody efficacy = 1 − Φ(a + b mAb) / Φ(a), where a and b are the maximum-likelihood estimates of A and B. The nonparametric bootstrap procedure was used to form confidence intervals for ID01 and antibody efficacy. All tests are two-sided, and *P* values less than 0.05 are considered significant.

Reporting Summary

Further information on experimental design is available in the Nature Research Reporting Summary linked to this article.

Data availability

The data sets generated and/or analyzed in supporting the findings of this study are available in the manuscript (and Supplementary Information). All other data are available from the corresponding authors on reasonable request.

References

1. Walker, L. M. et al. Broad neutralization coverage of HIV by multiple highly potent antibodies. *Nature* **477**, 466–470 (2011).

2. Walker, L. M. et al. Broad and potent neutralizing antibodies from an African donor reveal a new HIV-1 vaccine target. *Science* **326**, 285–289 (2009).

3. Wu, X. et al. Rational design of envelope identifies broadly neutralizing human monoclonal antibodies to HIV-1. *Science* **329**, 856–861 (2010).

4. Liao, H. X. et al. Co-evolution of a broadly neutralizing HIV-1 antibody and founder virus. *Nature* **496**, 469–476 (2013).

5. Scheid, J. F. et al. Sequence and structural convergence of broad and potent HIV antibodies that mimic CD4 binding. *Science* **333**, 1633–1637 (2011).

6. Sok, D. et al. Recombinant HIV envelope trimer selects for quaternary-dependent antibodies targeting the trimer apex. *Proc. Natl. Acad. Sci. USA* **111**, 17624–17629 (2014).

7. Garces, F. et al. Structural evolution of glycan recognition by a family of potent HIV antibodies. *Cell* **159**, 69–79 (2014).

8. Mouquet, H. et al. Complex-type N-glycan recognition by potent broadly neutralizing HIV antibodies. *Proc. Natl. Acad. Sci. USA* **109**, E3268–E3277 (2012).

9. Huang, J. et al. Broad and potent neutralization of HIV-1 by a gp41-specific human antibody. *Nature* **491**, 406–412 (2012).

10. Huang, J. et al. Broad and potent HIV-1 neutralization by a human antibody that binds the gp41–gp120 interface. *Nature* **515**, 138–142 (2014).

11. Scharf, L. et al. Antibody 8ANC195 reveals a site of broad vulnerability on the HIV-1 envelope spike. *Cell Reports* **7**, 785–795 (2014).

12. Gautam, R. et al. A single injection of anti-HIV-1 antibodies protects against repeated SHIV challenges. *Nature* **533**, 105–109 (2016).

13. Gruell, H. et al. Antibody and antiretroviral preexposure prophylaxis prevent cervicovaginal HIV-1 infection in a transgenic mouse model. *J. Virol.* **87**, 8535–8544 (2013).

14. Hessell, A. J. et al. Early short-term treatment with neutralizing human monoclonal antibodies halts SHIV infection in infant macaques. *Nat. Med.* **22**, 362–368 (2016).

15. Saunders, K. O. et al. Sustained delivery of a broadly neutralizing antibody in nonhuman primates confers long-term protection against simian/human immunodeficiency virus infection. *J. Virol.* **89**, 5895–5903 (2015).

16. Shingai, M. et al. Passive transfer of modest titers of potent and broadly neutralizing anti-HIV monoclonal antibodies block SHIV infection in macaques. *J. Exp. Med.* **211**, 2061–2074 (2014).

17. Moldt, B. et al. Highly potent HIV-specific antibody neutralization in vitro translates into effective protection against mucosal SHIV challenge in vivo. *Proc. Natl. Acad. Sci. USA* **109**, 18921–18925 (2012).

18. Barouch, D. H. et al. Therapeutic efficacy of potent neutralizing HIV-1-specific monoclonal antibodies in SHIV-infected rhesus monkeys. *Nature* **503**, 224–228 (2013).

19. Nishimura, Y. et al. Early antibody therapy can induce long-lasting immunity to SHIV. *Nature* **543**, 559–563 (2017).

20. Shingai, M. et al. Antibody-mediated immunotherapy of macaques chronically infected with SHIV suppresses viraemia. *Nature* **503**, 277–280 (2013).

21. Julg, B. et al. Virological control by the CD4-binding site antibody N6 in simian–human immunodeficiency virus–infected rhesus monkeys. *J. Virol.* **91**, e00498–17 (2017).

22. Caskey, M. et al. Viraemia suppressed in HIV-1-infected humans by broadly neutralizing antibody 3BNC117. *Nature* **522**, 487–491 (2015).

23. Caskey, M. et al. Antibody 10-1074 suppresses viremia in HIV-1-infected individuals. *Nat. Med.* **23**, 185–191 (2017).

24. Ledgerwood, J. E. et al. Safety, pharmacokinetics and neutralization of the broadly neutralizing HIV-1 human monoclonal antibody VRC01 in healthy adults. *Clin. Exp. Immunol.* **182**, 289–301 (2015).

25. Lynch, R. M. et al. Virologic effects of broadly neutralizing antibody VRC01 administration during chronic HIV-1 infection. *Sci. Transl. Med.* **7**, 319ra206 (2015).

26. Bar, K. J. et al. Effect of HIV antibody VRC01 on viral rebound after treatment interruption. *N. Engl. J. Med.* **375**, 2037–2050 (2016).

27. Scheid, J. F. et al. HIV-1 antibody 3BNC117 suppresses viral rebound in humans during treatment interruption. *Nature* **535**, 556–560 (2016).

28. Ko, S. Y. et al. Enhanced neonatal Fc receptor function improves protection against primate SHIV infection. *Nature* **514**, 642–645 (2014).

29. Halper-Stromberg, A. et al. Broadly neutralizing antibodies and viral inducers decrease rebound from HIV-1 latent reservoirs in humanized mice. *Cell* **158**, 989–999 (2014).

30. Klein, F. et al. HIV therapy by a combination of broadly neutralizing antibodies in humanized mice. *Nature* **492**, 118–122 (2012).

31. Advisory Committee on Immunization Practices. Prevention of hepatitis A through active or passive immunization: recommendations of the Advisory Committee on Immunization Practices (ACIP). *MMWR Recomm. Rep.* **55**, 1–23 (2006).

32. Pereyra, F. et al. The major genetic determinants of HIV-1 control affect HLA class I peptide presentation. *Science* **330**, 1551–1557 (2010).

33. Simek, M. D. et al. Human immunodeficiency virus type 1 elite neutralizers: individuals with broad and potent neutralizing activity identified by using a high-throughput neutralization assay together with an analytical selection algorithm. *J. Virol.* **83**, 7337–7348 (2009).

34. Shingai, M. et al. Most rhesus macaques infected with the CCR5-tropic SHIV(AD8) generate cross-reactive antibodies that neutralize multiple HIV-1 strains. *Proc. Natl. Acad. Sci. USA* **109**, 19769–19774 (2012).

35. Gautam, R. et al. Pathogenicity and mucosal transmissibility of the R5-tropic simian/human immunodeficiency virus SHIV(AD8) in rhesus macaques: implications for use in vaccine studies. *J. Virol.* **86**, 8516–8526 (2012).

36. Nishimura, Y. et al. Generation of the pathogenic R5-tropic simian/human immunodeficiency virus SHIVAD8 by serial passaging in rhesus macaques. *J. Virol.* **84**, 4769–4781 (2010).

Acknowledgements

We thank R. Plishka, A. Peach, P. King and O. Abegunrin for determining plasma viral RNA loads and R. Engel, R. Petros, Nero Ramera, B. Ahlin and M. Boursiquot for diligently assisting in the maintenance of animals and assisting with procedures. We thank National Institutes of Health (NIH) AIDS Research and Reference Reagent Program for TZM-bl and HEK293 T cells. This work was supported by the Intramural Research Program of the National Institute of Allergy and Infectious Diseases, NIH. The research was also funded in part by the Bill and Melinda Gates Foundation Collaboration for AIDS Vaccine Discovery Grants OPP1033115 and OPP1092074 (to M.C.N.) and by the NIH under award numbers AI-100148 and UM1 AI100663-01. M.C.N. is supported by the Robertson Foundation and Howard Hughes Medical Institute.

Author information

Affiliations

Laboratory of Molecular Microbiology, National Institute of Allergy and Infectious Diseases, National Institutes of Health, Bethesda, MD, USA
Rajeev Gautam, Yoshiaki Nishimura, Natalie Gaughan, Alicia Buckler-White & Malcolm A. Martin

Laboratory of Molecular Immunology, Rockefeller University, New York, NY, USA
Anna Gazumyan, Till Schoofs & Michel C. Nussenzweig

Center for Virology and Vaccine Research, Beth Israel Deaconess Medical Center, Boston, MA, USA

Michael S. Seaman

Biostatistics Research Branch, Division of Clinical Research, National Institute of Allergy and Infectious Diseases, National Institutes of Health, Bethesda, MD, USA
Bruce J. Swihart & Dean A. Follmann

Howard Hughes Medical Institute, Rockefeller University, New York, NY, USA
Michel C. Nussenzweig

Contributions

R.G., M.A.M. and M.C.N. designed experiments and wrote the manuscript; R.G., Y.N., N.G., A.G., A.B.-W. and M.S.S. performed experiments; R.G., Y.N., M.A.M., M.C.N., M.S.S., T.S., B.J.S. and D.A.F. analyzed data.

Corresponding authors

Correspondence to Michel C. Nussenzweig or Malcolm A. Martin.

Ethics declarations

Competing interests

The authors declare no competing interests.

Additional information

Publisher's note: Springer Nature remains neutral with regard to jurisdictional claims in published maps and institutional affiliations.

Electronic supplementary material

Supplementary Tables and Figures - ***https://static-content.springer.com/esm/art%3A10.1038%2Fs41591-018-0001-2/MediaObjects/41591_2018_1_MOESM1_ESM.pdf***
Supplementary Figures 1–3 and Supplementary Tables 1–3

Reporting Summary - ***https://static-content.springer.com/esm/art%3A10.1038%2Fs41591-018-0001-2/MediaObjects/41591_2018_1_MOESM2_ESM.pdf***

Rights and permissions

About this article

Cite this article

Gautam, R., Nishimura, Y., Gaughan, N. *et al.* A single injection of crystallizable fragment domain–modified antibodies elicits durable protection from SHIV infection. *Nat Med* **24,** 610–616 (2018). https://doi.org/10.1038/s41591-018-0001-2

Received03 October 2017Accepted09 February 2018Published16 April 2018

Issue DateMay 2018DOIhttps://doi.org/10.1038/s41591-018-0001-2

Further reading

Broadly neutralizing antibodies for HIV-1: efficacies, challenges and opportunities - ***https://doi.org/10.1080/22221751.2020.1713707***
Yubin Liu, Wei Cao, Ming Sun[…]Taisheng Li

Emerging Microbes & Infections (2020)

Broadly Neutralizing Antibodies for HIV Prevention - ***https://doi.org/10.1146/annurev-med-110118-045506***
Shelly T. Karuna & Lawrence Corey

Annual Review of Medicine (2020)

Optimization and qualification of a functional anti-drug antibody assay for HIV-1 bnAbs - ***https://doi.org/10.1016/j.jim.2020.112736***
Michael S. Seaman, Miroslawa Bilska, Fadi Ghantous, Amanda Eaton, Celia C. LaBranche, Kelli Greene, Hongmei Gao, Joshua A. Weiner, Margaret E. Ackerman, David A. Garber, Yvonne J. Rosenberg,

Marcella Sarzotti-Kelsoe[…]David C. Montefiori

Journal of Immunological Methods (2020)

openPrimeR for multiplex amplification of highly diverse templates -
https://doi.org/10.1016/j.jim.2020.112752
Christoph Kreer, Matthias Döring, Nathalie Lehnen, Meryem S. Ercanoglu, Lutz Gieselmann, Domnica Luca, Kanika Jain, Philipp Schommers, Nico Pfeifer[…]Florian Klein

Journal of Immunological Methods (2020)

Framework Mutations of the 10-1074 bnAb Increase Conformational Stability, Manufacturability, and Stability While Preserving Full Neutralization Activity -
https://doi.org/10.1016/j.xphs.2019.07.009
Bruce A. Kerwin, Chelsey Bennett, Yan Brodsky, Rutilio Clark, J. Alaina Floyd, Alison Gillespie, Bryan T. Mayer, Megan McClure, Christine Siska, Michael S. Seaman, Kelly E. Seaton, Jeremy Shaver, Georgia D. Tomaras, Nicole L. Yates[…]Randal R. Ketchem

Journal of Pharmaceutical Sciences (2020)

Nature Medicine

ISSN 1546-170X (online)